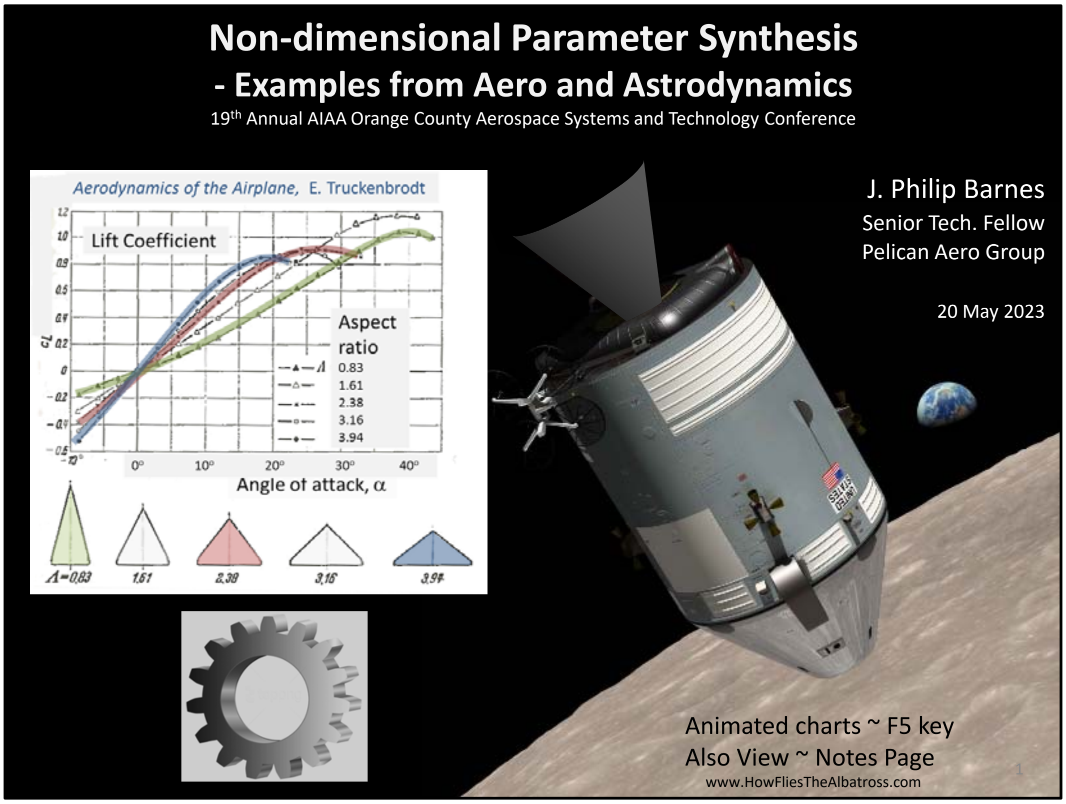

Non-dimensional parameters provide insightful and compact characterization of myriad physical phenomena. Over a century after its publication, Lord Rayleigh's "similitude" method of *dimensional analysis* remains powerful and relevant, perhaps with applications to the emerging science of artificial intelligence. And three centuries after the publication of *Principia*, Isaac Newton's gravitation and conic-section orbits continue big roles in our lives.

This presentation reviews and renews the synthesis and application of non-dimensional parameters, including for illustration empirical or theoretical characterization of wing aerodynamic lift, gear aerodynamic windage, and conic-section or Keplerian orbits. Throughout the presentation we'll describe the interesting physics of the chosen phenomena as we borrow from, and build upon, the work of Rayleigh and Newton.

Presentation Contents

- Introduction to non-dim. params.

- Rayleigh's "Similitude" method
  - Elegant and empirical synthesis
    - Both "art and science" aspects
  - Applied: Wing aerodynamic lift
  - Applied: Gear aero windage

- Newton's conic-section orbits
  - Tangent: Isaac Newton chronology
  - Analytical synthesis of parameters
  - Applied: "Patched-conic" Lunar trip

Wellcome Library, London

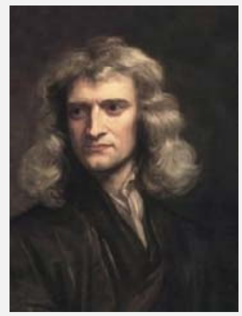

The presentation describes two methods to derive and/or apply non-dimensional parameters to efficiently and insightfully characterize physical phenomena. These methods can be named *empirical or analytical.* We'll first review and renew Rayleigh's *similitude* method of finding empirical exponents. We'll then coast, in more ways than one, as we review and renew Newton's conic-section orbits, applying the *patched-conic approximation* to study the Apollo *lunar free-return trajectory*.

Introduction to Non-dimensional Characterization

- Compact characterization of physical phenomena
  - Prevent exponential growth of the test matrix
- Avoid "Mars Lander" mixed and/or ambiguous units
- Two or more variables form a non-dimensional group
- Simple example: circle circumference & diam., $\pi \equiv C/D$
- Well-known example: Reynolds number $\equiv \rho vc/\mu$
  - fluid density (ρ), velocity (v), length (c), & viscosity (μ)
- *Myriad* applications (some below included herein):
  - Motor-generator torque, speed, & current[1]
  - Aerodynamic lift and drag coefficients
  - Conic-orbital position, velocity, and time[2]
  - Gear geometry, mesh loss, & windage[3]
  - Dynamic-soaring flight mechanics[4]
  - Heat transfer[3], tribology, ...

1 Barnes, J.P., AIAA 2016-4711, *Principles of High-efficiency Electric Flight*, 2016
2 Barnes, J.P., AAS 87-537, *Relating Conic-section Orbital Position, Velocity and Time From Periapsis as Dimensionless Quantities*, 1987
3 Barnes, J.P., AGMA 97FTM11, *Non-dimensional Characterization of Gear Geometry, Mesh Loss, and Windage*, 1997
4 Barnes, J.P., SAE 2004-01-3088, *How Flies the Albatross - the Flight Mechanics of Dynamic Soaring*, 2004

Non-dimensional parameters offer many benefits, including compact characterization. Consider a test matrix with just two variables, both of which may have non-linear effects. This may require up to eight test points to characterize, and if necessary modestly extrapolate, the test results. Then adding more variables the test matrix grows exponentially. Taking advantage of non-dimensional parameters, the test matrix remains comprehensive with far greater economy.

Perhaps the world's oldest, well-known dimensionless parameter is "π" representing of course a circle's circumference-to-diameter ratio. A relatively modern parameter is the Reynolds number, affecting fluid dynamics and heat transfer. Myriad applications of non-dimensional parameters include the three studies in this presentation.

Presentation Contents

- Introduction to non-dim. params.
- Rayleigh's "Similitude" method
  - Elegant and empirical synthesis
    - Both "art and science" aspects
  - Applied: Wing aerodynamic lift
  - Applied: Gear aero windage
- Newton's conic-section orbits
  - Tangent: Isaac Newton chronology
  - Analytical derivation of params.
  - Applied: "Patched-conic" Lunar trip

Wellcome Library, London

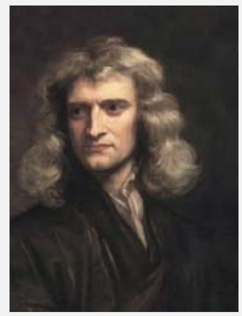

Rayleigh’s “Similitude” parameter synthesis

Application: *Empirical* study of wing aerodynamic lift

Assume lift (L) depends on angle of attack (α), mid-chord sweep (Λ), air density (ρ), airspeed (v), air viscosity (μ), speed of sound (a), span (b), and average chord (c).

Rayleigh’s **Principle of Similitude** (*Nature*, 1915) would suggest:

$$L = f(\alpha, \Lambda, \rho, \mathrm{v}, \mathrm{b}, \mu, \mathrm{a}, \mathrm{c}) \approx e_o\ \rho^{e_1}\ \mathrm{v}^{e_2}\ \mathrm{b}^{e_3}\ \mu^{x_1}\ \mathrm{a}^{x_2}\ \mathrm{c}^{x_3}$$

Exclude for now already-dimensionless terms (α, Λ)
Arbitrarily select (ρ, v, b) as “primary affectors,” with a non-singular units matrix for “auxiliary affectors” (μ, a, c) ; Then solve for the “auxiliary” exponents (x_i) in terms of the yet-unknown empirical exponents (e_i) so that Rayleigh’s formula obtains dimensions of lift

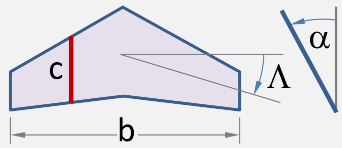

unit	ρ	v	b	μ	a	c	L
kg	1	0	0	1	0	0	1
m	-3	1	1	-1	1	1	1
s	0	-1	0	-1	-1	0	-2

www.HowFliesTheAlbatross.com 5

Rayleigh’s “similitude” method, circa 1915, condenses typically six *dimensional* “affectors”* into three *non-dimensional* groups. This dramatically reduces the scope of test data needed to empirically characterize the system at hand. Rayleigh postulates that a “keystone” entity (aero lift in the present example) is proportional to a series product of all suspected affectors, each raised to some exponent, such that the series product obtains the same units as the keystone entity. Typically three affectors together including units of mass, length, and time are arbitrarily selected as “primary” and three others then as “secondary or auxiliary.” If a temperature difference applies it becomes a fourth auxiliary affector. Later operations allow optional re-arrangement to draw from experience and the “artistic” aspect of the method’s “art and science” duality.

A units table is constructed, as shown above, and the “auxiliary” portion thereof must represent a non-singular rank-3 or rank-4 matrix. Subsequent matrix operations then solve for the auxiliary exponents (x_i) in terms of the yet-unknown empirical exponents (e_i). Test data then reveals the typically non-integer empirical exponents. Often the empirical *factor* (e_o) plays no visible role, as herein for our study of gear aero windage.

The “renew” aspects of our “review” of Rayleigh’s method include distinguishing primary from secondary entities, demonstration of matrix operations, and introduction of “artistic” operations, including group re-arrangement options and ways to handle already-dimensionless affectors, in this case (α, Λ).

* Not to be confused with the medical term “effector”

Rayleigh's "Similitude" dimensional analysis, continued 1

Application: *Empirical* study of wing aerodynamic lift

To ensure dimensional consistency, arrange all exponents in a set of equations, one for each applicable unit (kg, meter, sec):

	ρ		v		b		μ		a		c		L
kg:	$(1)\,e_1$	+	$(0)\,e_2$	+	$(0)\,e_3$	+	$(1)\,x_1$	+	$(0)\,x_2$	+	$(0)\,x_3$	=	1
m:	$(-3)\,e_1$	+	$(1)\,e_2$	+	$(1)\,e_3$	+	$(-1)\,x_1$	+	$(1)\,x_2$	+	$(1)\,x_3$	=	1
s:	$(0)\,e_1$	+	$(-1)\,e_2$	+	$(0)\,e_3$	+	$(-1)\,x_1$	+	$(-1)\,x_2$	+	$(0)\,x_3$	=	-2

Re-write as [A] [x] = [B] to solve for auxiliary exponents $[x_i]$ in terms of $[e_i]$:

$$\begin{pmatrix} 1 & 0 & 0 \\ -1 & 1 & 1 \\ -1 & -1 & 0 \end{pmatrix} \begin{pmatrix} x_1 \\ x_2 \\ x_3 \end{pmatrix} = \begin{pmatrix} 1 - e_1 \\ 1 + 3\,e_1 - e_2 - e_3 \\ -2 + e_2 \end{pmatrix}$$

Invert [A] and write $[x]=[A^{-1}][B]$:

$$\begin{pmatrix} x_1 \\ x_2 \\ x_3 \end{pmatrix} = \begin{pmatrix} 1 & 0 & 0 \\ -1 & 0 & -1 \\ 2 & 1 & 1 \end{pmatrix} \begin{pmatrix} 1 - e_1 \\ 1 + 3\,e_1 - e_2 - e_3 \\ -2 + e_2 \end{pmatrix} = \begin{pmatrix} 1 - e_1 \\ 1 + e_1 - e_2 \\ 1 + e_1 - e_3 \end{pmatrix}$$

Here the units table of the previous slide has been represented by a system of equations representing all lift affectors and exponents, with the units of lift represented by the column vector at upper right. This system is then converted to matrix form and the auxiliary units matrix (middle-left) is inverted to solve for the auxiliary exponents (x_i) in terms of the empirical exponents (e_i), acknowledging that the empirical exponents are not yet known.

Rayleigh's "Similitude" dimensional analysis, continued 2

Application: *Empirical* study of wing aerodynamic lift

Recall the original assertion:

$$L = f(\alpha, \Lambda, \rho, v, b, \mu, a, c) = e_o\, \rho^{e_1}\, v^{e_2}\, b^{e_3}\, \mu^{x_1}\, a^{x_2}\, c^{x_3}$$

Recall from the previous slide:

$$\begin{pmatrix} x_1 \\ x_2 \\ x_3 \end{pmatrix} = \begin{pmatrix} 1 - e_1 \\ 1 + e_1 - e_2 \\ 1 + e_1 - e_3 \end{pmatrix}$$

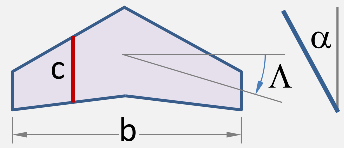

Three right-hand groups characterize the left-hand group. We now add in angle of attack (α), as a fourth dimensionless right-hand "group"

$$\frac{L}{\mu\ a\ c} = e_o \left[\frac{\rho a c}{\mu}\right]^{e_1} \left[\frac{v}{a}\right]^{e_2} \left[\frac{b}{c}\right]^{e_3} [\alpha]^{e_4}$$

Interesting, but not fully satisfactory ; Next, draw more upon the "artistic" aspect of the method

Now combining the auxiliary exponent solution with what would be Rayleigh's postulate yields three right-hand groups efficiently characterizing one left-hand group. Such groups, preliminary at this point, can be named a "pseudo" lift coefficient, pseudo Reynolds number, Mach number, and wing geometric aspect ratio (span/average_chord). Applying "art and experience," and/or perhaps separate test data or theory, we replace the geometric aspect ratio with its "equivalent aspect ratio," dividing by the cosine of the mid-chord sweep angle.*

We will next fine-tune the correlation, but before doing so we recall that any number raised to the 0th power becomes unity, whereby any dimensionless group having an empirical exponent near zero will thus have little or no effect on the lift group. Furthermore any non-zero empirical exponent may be negative, as with Reynolds number were we instead to characterize aerodynamic *drag*.

* Barnes, J.P., *Configuration Aerodynamics - Classical Methods Applied*, AIAA 2020-2708

Rayleigh's "Similitude" dimensional analysis, continued 3

Application: *Empirical* study of wing aerodynamic lift

"Art & science": *equivalent aspect ratio* includes sweep

$$\frac{\mathrm{L}}{\mu\ \mathrm{a}\ \mathrm{c}} = e_o \left[\frac{\rho \mathrm{ac}}{\mu}\right]^{e_1} \left[\frac{\mathrm{v}}{\mathrm{a}}\right]^{e_2} \left[\frac{\mathrm{b/c}}{cos\Lambda}\right]^{e_3} [\alpha]^{e_4}$$

Factor by (a/v) ; then divide by (1/2) [ρvc/μ] [b/c]

$$\frac{2\mathrm{L}}{\rho\ \mathrm{v}^2\ \mathrm{bc}} = e_o \left[\frac{\rho \mathrm{vc}}{\mu}\right]^{e_1} \left[\frac{\mathrm{v}}{\mathrm{a}}\right]^{e_2} \left[\frac{\mathrm{b/c}}{cos\Lambda}\right]^{e_3} \alpha^{e_4}$$

Lift coefficient	Reynolds number	Mach number	Aspect ratio	AoA

$e_o \sim 0.017$; $e_1 \sim 0$; $e_2 \sim 0$; $e_3 \sim 0.85$; $e_4 \sim 1$

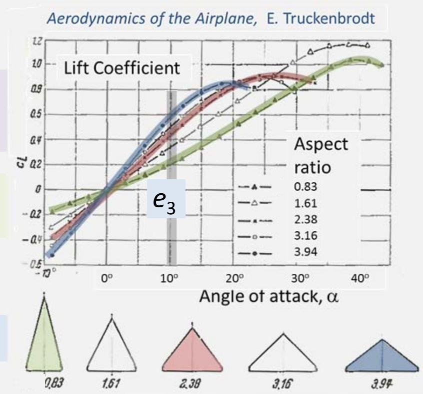

Our calculations thus far yielded a "pseudo" Reynolds number which we may argue is known from previous studies to be based on airspeed (v), and not the speed of sound (a). Here, we are at liberty to invert every ratio (a/v) or (b/c). We are also at liberty to factor or divide both sides of the equation by any single or group entity. Strictly speaking, such factoring or dividing both sides by any group adds or subtracts unity to the empirical exponent for that group. However, we can more conveniently allow all empiricals (e_i) to "float" unchanged for now, but soon to be revealed empirically. Provided the data is taken above a *critical Reynolds number*, and below a *critical Mach number*, where neither is found to affect lift, we discover the two related empirical exponents to be zero.

To isolate the empirical exponent (e_3), we cross plot test data (lower right) for lift coefficient (linear range) versus equivalent aspect ratio. Next, we observe that the exponent on angle of attack is unity. Finally, the empirical factor (e_o) is revealed by inspection to fit the test data. We thus emerge with a compact mathematical model of low-aspect-ratio, swept-wing lift within stated limits. But the method also "warns" us of possible regimes where changes in Reynolds or Mach number may affect lift. Indeed, these appear at transonic Mach number and/or at "model aircraft" Reynolds numbers.

Presentation Contents

- Introduction to non-dim. params.
- Rayleigh's "Similitude" method
  - Elegant and empirical synthesis
    - Both "art and science" aspects
  - Applied: Wing aerodynamic lift
  - Applied: Gear aero windage
- Newton's conic-section orbits
  - Tangent: Isaac Newton chronology
  - Analytical derivation of params.
  - Applied: "Patched-conic" Lunar trip

Wellcome Library, London

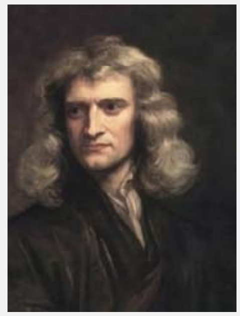

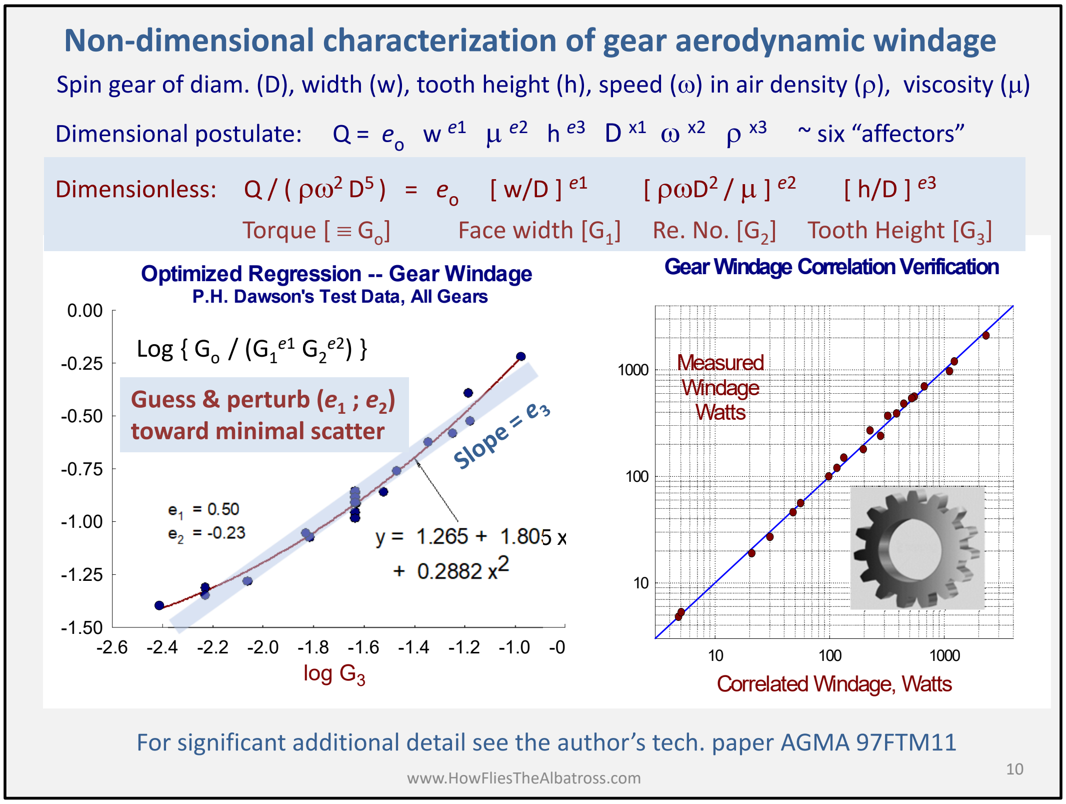

Having applied Rayleigh's method to a relatively-simple case, we now apply it to a case exhibiting more typical complexities. The present example characterizes gear aerodynamic "windage" or torque required to spin the gear in a gaseous atmosphere such as dry air. Rayleigh's method condenses six affectors of windage into three non-dimensional groups [G_1 G_2 G_3] which, with their empirical exponents (e_1 e_2 e_3), characterize the non-dimensional windage torque group [G_o]. The affectors are gear diameter, rotational speed, tooth height, tooth width, air density, and air viscosity.

We have test data for all the dimensionless groups, but we do not yet know the three empirical exponents corresponding to the three right-hand groups. Our suggested and applied approach guesses with systematic variation the empirical exponents (e_1 e_2) which combined with [G_o G_1 G_2] isolate, with a certain amount of scatter to be minimized, the effects of [G_3]. Typically such exponents are less than unity, but Reynolds number will have a negative exponent thereof. At the lower right the final correlation exhibits a very good match to the test data. Curiously, the postulated empirical factor (e_o) makes no obvious appearance, apparently "buried" in the result.

Presentation Contents

- Introduction to non-dim. params.
- Rayleigh's "Similitude" method
  - Elegant and empirical synthesis
    - Both "art and science" aspects
  - Applied: Wing aerodynamic lift
  - Applied: Gear aero windage
- Newton's conic-section orbits
  - Tangent: Isaac Newton chronology
  - Analytical synthesis of parameters
  - *Patched-conic* lunar free-return traj.

Wellcome Library, London

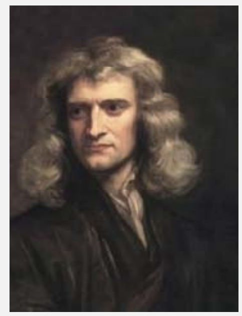

www.HowFliesTheAlbatross.com

11

Conic-section orbits: Isaac Newton Chronology

Year	Age	Development or Event
1665	23	Trinity math degree, avoids plague
1665	23	Invents differential calculus
1666	24	Invents Integr. calculus & gravitation
1668	26	Cambridge faculty appointment
1672	30	Elected Royal Society Fellow
1684	42	Leibniz invents/publishes calculus
1685	43	Sphere point-mass equivalent
1686	44	Book: *Principia* (proofs geometric)
1702	60	Newton publishes his own calculus
1708	66	Knighted
1727	85	Quoted, shortly before death:

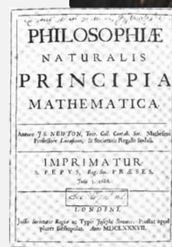
PHILOSOPHIÆ
NATURALIS
PRINCIPIA
MATHEMATICA
IMPRIMATUR

"*I do not know what I may appear to the world, but to myself I seem to have been only like a boy playing on the seashore, and diverting myself in now and then finding a smoother pebble or a prettier shell than ordinary, while the great ocean of truth lay all undiscovered before me*."

www.HowFliesTheAlbatross.com

12

Isaac Newton entered college with little or no knowledge of mathematics, and graduated at age 23 from Trinity as a supreme master of the discipline. Based on his work at Trinity and at home in Lincolnshire, where he retreated to avoid the plague, he invented differential calculus in his first year out of college. The next year he invented integral calculus[7], and his concept for gravitation. Secretive and socially dysfunctional[8,9], Newton originally kept his calculus to himself, and in publishing his epochal book *Principia* at the age of 44, employed entirely geometric proofs. Only well after Leibniz[10] independently discovered and published calculus did Newton reveal his own calculus, via his book *Optix*, at the age of 60. Nevertheless, Newton's mastery of geometric proofs in *Principia,* explaining numerous phenomena including conic-orbital shapes, orbital times, and earth-moon effects, remains today arguably unparalleled[11]. Newton's legacy is marred by his accusing Leibniz of plagiarizing calculus and by his refusal to support awarding a prize well earned by John Harrison for invention of the first clock of sufficient accuracy to enable accurate determination of longitude at sea.

07 Gamow, G., *The Great Physicists From Galileo to Einstein*, Dover, 1988

08 Jardine, L., *Ingenious Pursuits, Building the Scientific Revolution*, Anchor, 2000

09 Hawking, S.W., *A Brief History of Time*, Bantam, p. 181-182

10 Singer, C., A Short History of Science to the Nineteenth Century, Dover 1997

11 F.R. Moulton, *Introduction to Celestial Mechanics*, Dover, 1970, p.67,97,190

Conic-section orbits: From *Principia* to the present day

"... if any body is acted upon by a...force that is inversely proportional to the square of the distance...from the center, this body will move in...one of the conics having a focus in the center of forces."
Newton, *Principia,* Book 1, Section 3, 1686

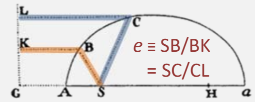

Conic section, Principia, Book 1, Section 4, 1686

Symbols and Definitions

- μ Product of central mass (M) & universal gravitational constant (G)
- r Radius from the central body center to the satellite
- θ True anomaly (angle from closest passage)
- v Satellite velocity relative to the central body
- γ Flight path angle (see sketch)
- h Angular momentum per unit satellite mass
- t Time from periapsis (closest passage)
- ε Total kinetic & potential energy per unit satellite mass
- *e* Eccentricity of conic section (*italic* Vs. natural-log base, e)

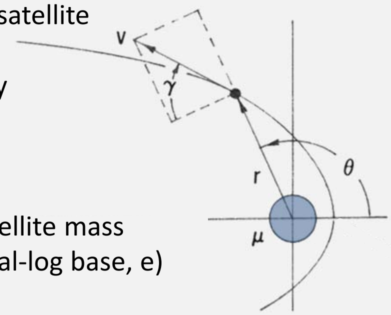

www.HowFliesTheAlbatross.com 13

Newton stated in *Principia* that any body acted upon solely by a force inversely proportional to the square of the distance from the force center would travel along one of the conics, with the force center residing at the conic-section focus. At lower right we sketch a conic orbit annotated with contemporary nomenclature, and at lower left we list the various orbital quantities.

Analytical derivation of orbital non-dimensional parameters

Original Analysis by F.R. Moulton, 1914

Added herein:
- Velocity Vs. position
- Time from Periapsis
- Non-dimensional r,v,t
- *Kepler's Problem Sol'n*

$$\ddot{r} = -\frac{\mu}{r^2} + r\dot{\theta}^2$$

Substitutions, incl. $d\theta/dt = h/r^2$; conic-section definition, and diff. eqn.sol'n yield orbital shape:

$$\boxed{r = \frac{h^2}{\mu} / (1 + e\cos\theta)}$$

Also, $dt = \frac{r^2}{h} d\theta$ thus:

$$\boxed{t = \frac{h^3}{\mu^2}\int_0^\theta \frac{d\theta}{(1 + e\cos\theta)^2}}$$

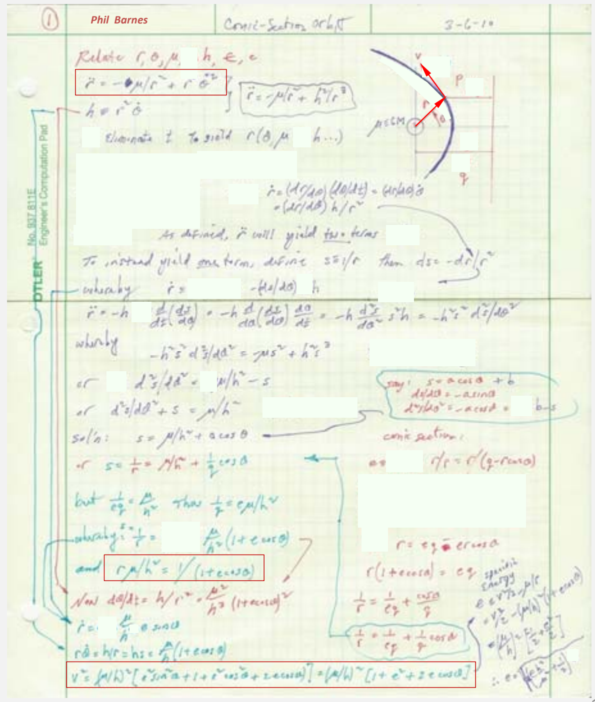

www.HowFliesTheAlbatross.com

14

Here we follow F. R. Moulton[11] to analytically derive conic-section orbital shape. Added to that is our own study of time from periapsis. The process begins with the radial acceleration formula, then applies various substitutions, recalls the definition of a conic section, and solves a differential equation, all yielding orbital radius versus position. Next we relate time and position with an equation which can be numerically or directly integrated. By inspection, the non-dimensional radius and time emerge when the two boxed equations at left are re-arranged for only eccentricity (e) and true anomaly (θ) to remain on the right-hand side. Further arithmetic, included in the author's hand-written notes at right, reveals the non-dimensional velocity and non-dimensional orbital energy.

[11] F.R. Moulton, *Introduction to Celestial Mechanics*, Dover, 1970 p. 80-82, 93, 67, 97, 190

Conic-section orbits: Dimensional & non-dimensional terms

Entity	Dimensional	Non-dimensional
Radius	$r = (h^2/\mu) / (1 + e\cos\theta)$	$R \equiv r\mu/h^2 = 1/(1 + e\cos\theta)$
Velocity	$v = \sqrt{2(\varepsilon + \mu/r)}$	$V \equiv vh/\mu = \sqrt{1 + e^2 + 2e\cos\theta}$
Flt. angle	$\gamma = \cos^{-1}[h/(rv)]$	$\gamma = \cos^{-1}[1/(RV)]$
Energy	$\varepsilon \equiv (v^2/2) - (\mu/r)$	$E \equiv \varepsilon\, h^2/\mu^2 = (V^2/2) - (1/R)$
	$\varepsilon = \mu^2(e^2 - 1)/(2h^2)$	$E = (e^2 - 1)/2$
Time	$t = (h^3/\mu^2)\int_0^\theta \frac{d\theta}{(1 + e\cos\theta)^2}$	$T \equiv \frac{t\mu^2}{2\pi h^3} = \frac{1}{2\pi}\int_0^\theta \frac{d\theta}{(1 + e\cos\theta)^2}$

For $e < 1$, the integral of the left side is (see Peirce, Short Table of Integrals,

$$T = \int_0^\theta \frac{[1/(2\pi)]\, d\theta}{(1 + e\cos\theta)^2} = \frac{[1/(2\pi)]}{1 - e^2}\left(\frac{-e\sin\theta}{1 + e\cos\theta} + \int_0^\theta \frac{d\theta}{1 + e\cos\theta}\right)$$

$$= \frac{[1/(2\pi)]}{1 - e^2}\left[\frac{-e\sin\theta}{1 + e\cos\theta} + \frac{2}{\sqrt{1 - e^2}}\tan^{-1}\left(\frac{\sqrt{1 - e^2}}{1 + e}\tan\tfrac{1}{2}\theta\right)\right]$$

For $e > 1$,

$$T = \int_0^\theta \frac{[1/(2\pi)]\, d\theta}{(1 + e\cos\theta)^2} = \frac{[1/(2\pi)]}{e^2 - 1}\left[\frac{e\sin\theta}{(1 + e\cos\theta)} - \frac{1}{\sqrt{e^2 - 1}}\ln\left(\frac{\sqrt{e+1} + \sqrt{e-1}\tan\frac{1}{2}\theta}{\sqrt{e+1} - \sqrt{e-1}\tan\frac{1}{2}\theta}\right)\right]$$

For $e = 1$,

$$T = \frac{3\tan(\frac{1}{2}\theta) + \tan^3(\frac{1}{2}\theta)}{12\pi}$$

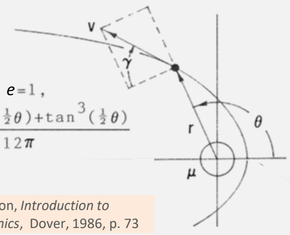

W.T. Thomson, *Introduction to Space Dynamics*, Dover, 1986, p. 73

www.HowFliesTheAlbatross.com

15

Together with Augenstein[12], Bate et.al.[13], and others we are motivated for various reasons to non-dimensionalize the orbital parameters. Our own formulation herein is unique in its simplicity and combined compact graphical characterization of elliptical and hyperbolic orbits together. Other motivations include dovetailing with the *patched-conic* method, expedited solution of Kepler's problem, and avoidance of mixed-unit scenarios (recall the Mars Lander failure).

At upper left we show the original dimensional quantities (r, v, ε, t). At upper are their non-dimensional counterparts (R, V, E, T), in terms of the eccentricity (*e*) and true anomaly (θ). As might be expected for a circular orbit (*e*=0) the non-dimensional radius (R), non-dimensional velocity (V), and non-dimensional period (T) are all unity.

To define non-dimensional time (T) from periapsis we can arbitrarily divide by (2π), making the circular orbital period unity. Our original paper (appended herein) had numerically integrated (T), but after its publication we learned that such can be directly integrated[14]. In the slide above, the time-related formulas are shown at lower left for elliptical and hyperbolic orbits, and at lower right for a parabolic orbit.

12 Augenstein, B.W., *Dynamics Problems With Satellite Orbit Control*, Trans. ASME, Nov. 1959
13 Bate, Mueller, White, *Fundamentals of Astrodynamics*, Dover, 1971, p. 41
14 Thomson, W.T., *Introduction to Space Dynamics*, Dover, 1986, p. 73

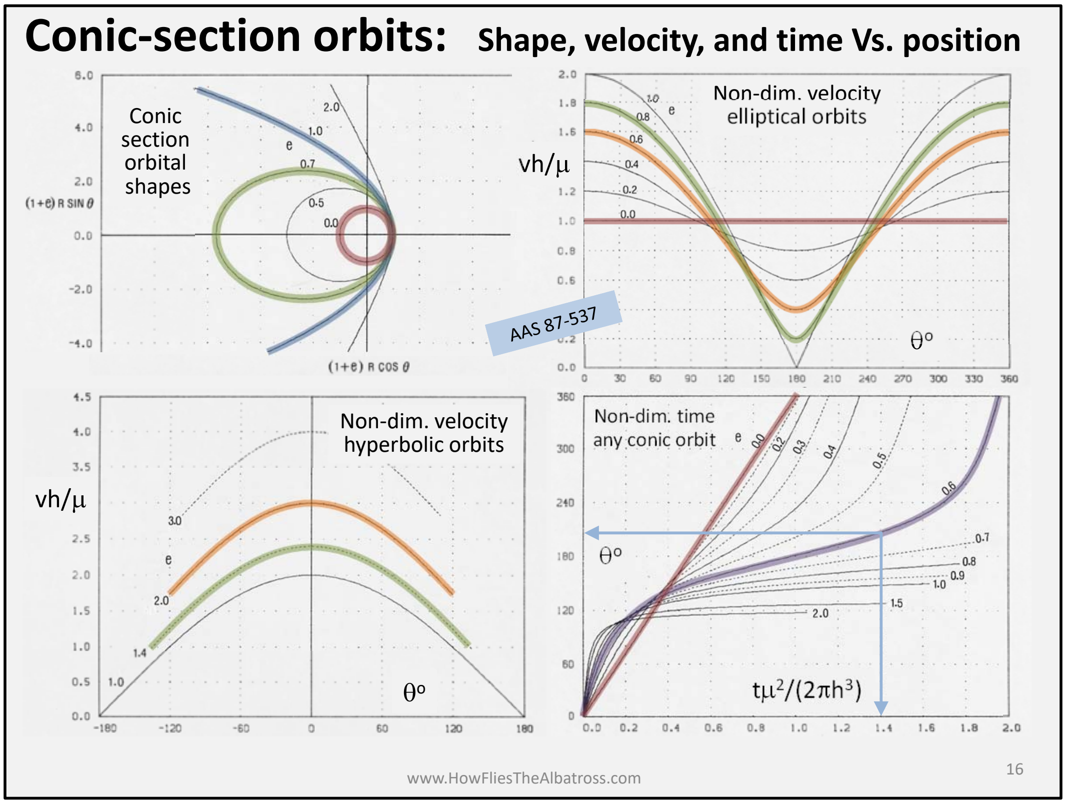

Here we show the non-dimensional shape, velocity, and time from periapsis for conic-section orbits. Again for the circular orbit, the non-dimensional radius, velocity, and period are all unity.

At lower right the non-dimensional time is presented as the independent parameter, although it has been calculated dependent on the eccentricity and true anomaly. This characterization, with either time or position taken as the independent variable, expedites conic orbital analysis, including the iterative solution of *Kepler's Problem*, to find the change in position, given the change in time.

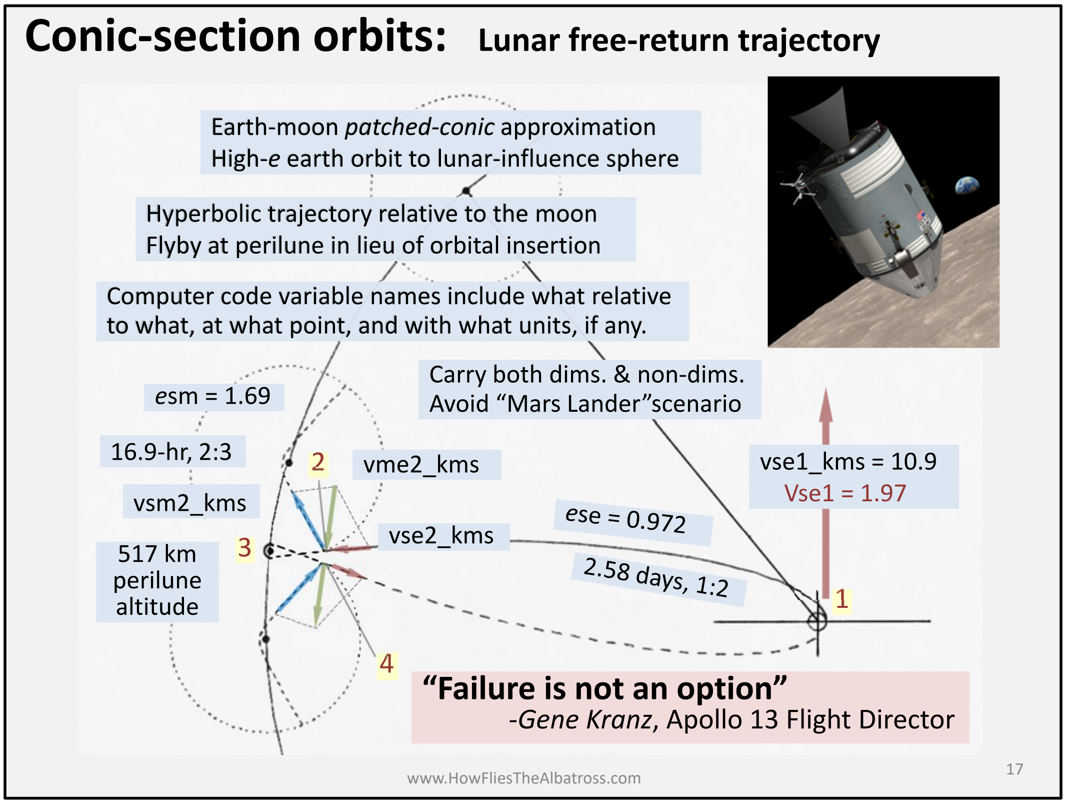

Here we apply Newton's conic-section orbits in the form of a *lunar free-return trajectory*[15] which, in taking the shape of a distorted but symmetrical figure-8, gives the astronauts a good chance of a safe return home in the event that the lunar-orbit-insertion (LOI) burn at perilune fails to happen. But the return trajectory does not by itself guarantee a safe return because of numerous other risks, for example the narrow window of an acceptable earth-atmospheric re-entry angle. The author's technical paper, embedded on slide 18 (AAS kept no record of it) applies the earth-moon orbit non-dimensional orbital parameters to analyze the trajectory. In this last chart we'll focus on handling also the *dimensional* terms in our computer code.

In the diagram above, with the orbital shape shown to scale, the spacecraft undergoes trans-lunar injection (TLI) at point-1 with a 6.5-min burn starting from a 300-km parking orbit. The spacecraft then coasts 2.58 days in a high-eccentricity (ese=0.972) earth orbit to reach the lunar sphere of influence (SOI) at point-2, where the spacecraft at moon-relative velocity (vsm2_kms) begins a hyperbolic passage of moon-relative eccentricity (esm=1.69). The spacecraft then travels 16.9-hr from SOI entry to perilune at point-3 where an optional multi-minute burn decelerates the spacecraft for lunar-orbit insertion (LOI).

If such burn does not happen, the spacecraft enters a free return to earth at point-4 whereby the spacecraft will have undergone a *gravitational flyby* at the special conditions which do not alter the earth-relative orbital energy of the spacecraft.

The analysis above applies the *patched-conic approximation* which has numerous opportunities for error accumulation. For example, the earth and moon together rotate about a common center of gravity which resides inside the earth at about ¾ of the earth's radius. In practice, the mission incorporates course corrections, typically including one at the point of entry into the lunar SOI. Without such correction, perilune altitude may differ from that desired.

An Apollo astronaut, orbiting the moon alone, was alarmed to perceive his spacecraft altitude at perilune to be below the highest peaks in the lunar terrain. He quickly advanced the throttle, but had not yet secured himself in a seat, whereby he found himself thrown to the back of the spacecraft as it accelerated[16]. Fortunately, he regained control. Spaceflight is often unforgiving, and beginning with orbital analysis, *failure is not an option*, to quote Apollo 13 Flight Director Gene Kranz.

15 Kaplan, M.H., *Modern Spacecraft Dynamics…, Wiley, 1976, p. 107*
16 Worden, A., *Falling to Earth, Smithsonian, p. 184-185*

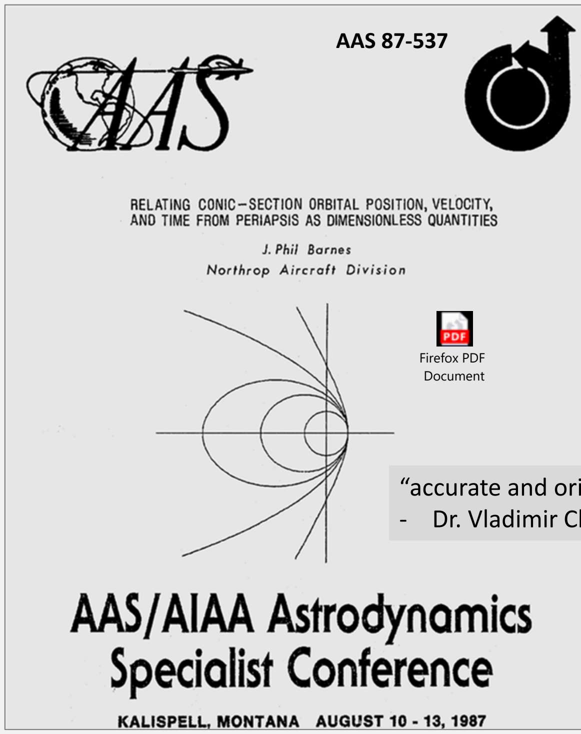
AAS 87-537

AAS

RELATING CONIC–SECTION ORBITAL POSITION, VELOCITY, AND TIME FROM PERIAPSIS AS DIMENSIONLESS QUANTITIES

J. Phil Barnes
Northrop Aircraft Division

AAS/AIAA Astrodynamics Specialist Conference

KALISPELL, MONTANA AUGUST 10 - 13, 1987

Firefox PDF Document

"accurate and original"
- Dr. Vladimir Chobotov

About the Author

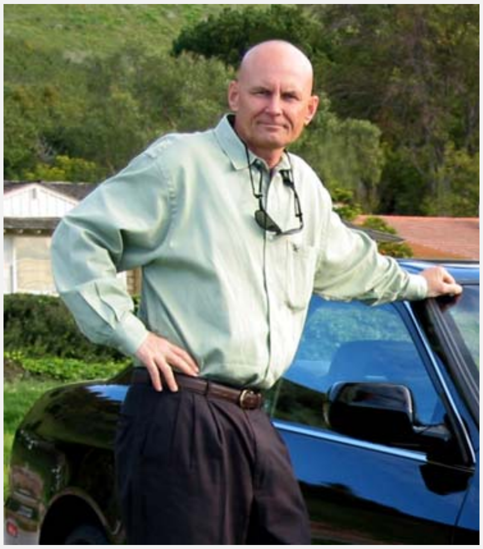

J. Philip “Phil” Barnes has a Master’s Degree in Aero Engineering from Cal Poly Pomona and Bachelors Degree in Mechanical Engineering from the Univ. of Arizona. He recently retired as a 40-year veteran of air vehicle and subsystems performance analysis at Northrop Grumman, supporting mature and advanced tactical aircraft programs. Author of a dozen technical papers, and often invited to deliver travel-paid lectures at various universities, Phil has mentored university teams working capstone projects; the fruits of such collaboration appear in his most recent work.

As one of the world’s top experts on albatross *dynamic soaring*, he is pioneering the science of *regenerative-electric flight*. Phil was nominated by Aviation Week’s Bill Sweetman and Phil’s academic network to deliver the AIAA 2020 von Karman lecture.

PAPER AAS 87-537

RELATING CONIC-SECTION ORBITAL POSITION, VELOCITY, AND TIME FROM PERIAPSIS AS DIMENSIONLESS QUANTITIES

J. Phil Barnes

Northrop Aircraft Division

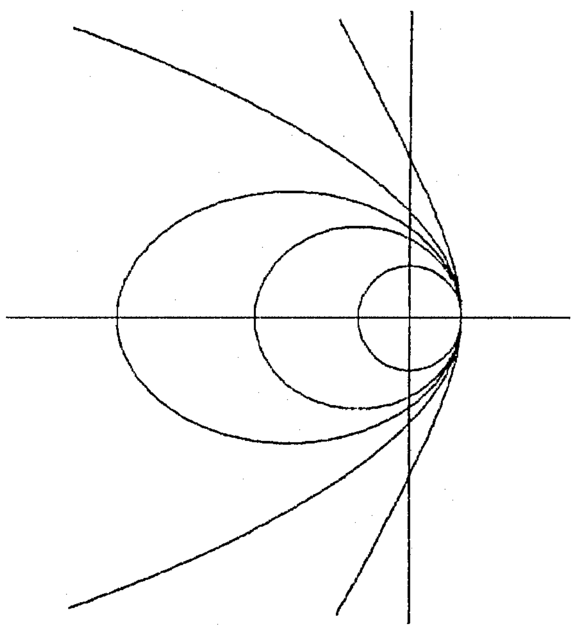

AAS/AIAA Astrodynamics Specialist Conference

KALISPELL, MONTANA AUGUST 10 - 13, 1987

AAS Publications Office, P.O. Box 28130, San Diego, CA 92128

RELATING CONIC-SECTION ORBITAL POSITION, VELOCITY, AND TIME FROM PERIAPSIS AS DIMENSIONLESS QUANTITIES

J. Phil Barnes*

Keplerian orbital characteristics are presented in compact mathematical and graphical form by non-dimensionalizing orbital radius, velocity, energy, and time from periapsis. The auxiliary anomalies are used to obtain the dimensionless time. The accuracies of the eccentric and hyperbolic anomalies are confirmed, particularly at near-parabolic eccentricity, by numerical solution of Kepler's problem. Finally, the dimensionless groups are applied toward analysis of a lunar free-return trajectory via the patched-conic method with the aid of Cartesian vector operations.

INTRODUCTION

A Keplerian orbit (Figure 1) has the shape of a conic section. The orbit is defined by its eccentricity (e), angular momentum (h) per unit satellite mass, and central body gravitational parameter (μ). The orbital radius (r), velocity (v), and time (t) from periapsis can be multiplied by various powers of (μ) and (h) to form dimensionless groups which, along with flight-path angle (γ), depend only on the eccentricity and true anomaly (θ). The orbital energy (ε) per unit satellite mass can also be non-dimensionalized.

Figure 1
Keplerian Orbital Parameters

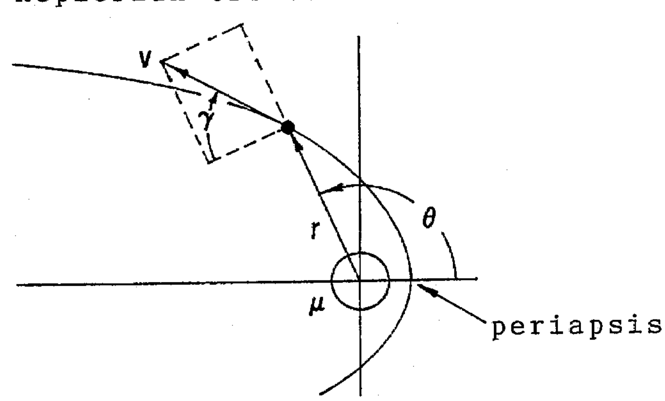

The dimensionless groups, derived in Appendix 1, are summarised as follows, using upper-case letters (R,V,E, and T) to designate non-dimensionality:

*Senior Engineer, Northrop Aircraft Division

Introduction, continued

Radius Group $R = r\mu/h^2 = 1/(1+ e\cos\theta)$

Velocity Group $V = vh/\mu = \sqrt{1+e^2+2\,e\cos\theta}$

Flight-Path Angle $\gamma = \cos^{-1}(1/RV)$

Energy Group $E = \mathcal{E}h^2/\mu^2 = \frac{1}{2}(V^2)-(1/R) = \frac{1}{2}(e^2-1)$

Time Group $T = t\mu^2/2\pi h^3 = (1/2\pi)\int_0^\theta \frac{d\theta}{(1+e\cos\theta)^2}$

Since the time-group integral cannot be evaluated by ordinary means (unless e=1), the eccentric anomaly (ϵ) and hyperbolic anomaly (F) were devised (Ref.1) as auxiliary anomalies which can be integrated. For eccentric, parabolic, and hyperbolic orbits, the time group is respectively as follows:

* After this paper was written, it was found that the time group can be integrated, as in Thomson's book, "Introduction to Space Mechanics," Dover, 1986, page 73.

For $e<1$, $$T = \frac{\epsilon - e\sin\epsilon}{2\pi(1-e^2)^{3/2}}$$

For $e=1$, $$T = \frac{3\tan(\frac{1}{2}\theta)+\tan^3(\frac{1}{2}\theta)}{12\pi}$$

For $e>1$, $$T = \frac{e\sinh(F) - F}{2\pi(e^2-1)^{3/2}}$$

With the auxiliary anomalies (ϵ, $\frac{1}{2}\theta$, or F) the solution of Kepler's problem (to determine θ, given T) is iterative. Also, when the eccentricity is near unity the iterative solutions are slow to converge and may be subject to error when (T) is evaluated in single precision. As an alternate, non-iterative solution to Kepler's problem, the dimensionless time derivative ($d\theta/dT$) can be integrated numerically:

$$d\theta/dT = 2\pi(1+e\cos\theta)^2 \longrightarrow \theta \approx \Sigma_0^T (d\theta/dT)\,\Delta T$$

The numerical integration can be used to test the accuracy of (T) as determined by the auxiliary anomalies. Also, numerical integration can be used as an alternative to the iterative methods when they are slow or unable to converge.

Regardless of how the time group (T) is obtained, the dimensionless groups (R,V,E, and T) offer compact presentation of orbital characteristics, as well as efficient analysis of conic and patched-conic orbits.

PRESENTATION OF ORBITAL CHARACTERISTICS

The orbital shapes can be compared by plotting dimensionless Cartesian coordinates, $X=R\cos\theta$ and $Y=R\sin\theta$, as shown in Figure 2. As might be expected, the circular orbit has a radius group of unity. At the semilatus nodes, all conic orbits have a radius group of unity. By scaling up the X-Y coordinates by the factor (1+e), the orbits can be compared with common periapsis as shown in Figure 3.

The velocity group, as well, is unity in a circular orbit (Figure 4). In eccentric orbits, the velocity group is (1+e) at periapsis and (1-e) at apoapsis. The direction of the velocity vector is given by the flight-path angle (γ), which varies with (e,θ) as shown in Figure 5. In hyperbolic orbits (Figure 6) the velocity group is again (1+e) at periapsis. The flight-path angle is linear with true anomaly for a parabolic orbit (Figure 7).

For eccentric, parabolic, and hyperbolic orbits the dimensionless time from periapsis (time group, T) is presented in Figure 8. Note that the dimensionless period of the circular orbit is unity. The time group arbitrarily contains (2π) in its definition, allowing convenient calcellation of the (2π) when converting radians to degrees in numerical or iterative solutions to Kepler's problem.

For eccentric orbits, the period (τ) and period group (P) are related as follows:

$$P = \tau\mu^2/2\pi h^3 = 1/(1-e^2)^{3/2}$$

Figure 9 relates the true anomaly to the time from periapsis as a fraction (t/τ) of the period.

In hyperbolic orbits (Figure 10) the time group is negative approaching periapsis. Figures 8 or 10 can be used for approximate graphical solution of Kepler's problem. Given an initial true anomaly (θ_1) along with the eccentricity, the initial time group (T_1) can be obtained graphically. Then, given (h) and (μ), the time interval (t_2-t_1) is non-dimensionalized to form (T_2-T_1). Then, given the final time group (T_2), the final true anomaly (θ_2) is obtained graphically.

Figures 8 or 10 also offer a close first guess for the final true anomaly in the iterative solution to Kepler's problem, as illustrated in Appendix 2. Since the iterative solution uses (e), (T), and the auxiliary anomaly to determine (θ), the velocity group ($V=vh/\mu$) is ideally suited for determining the dimensional velocity (v):

$$v = (\mu/h)\sqrt{1+e^2+2e\cos\theta}$$

Figure 2

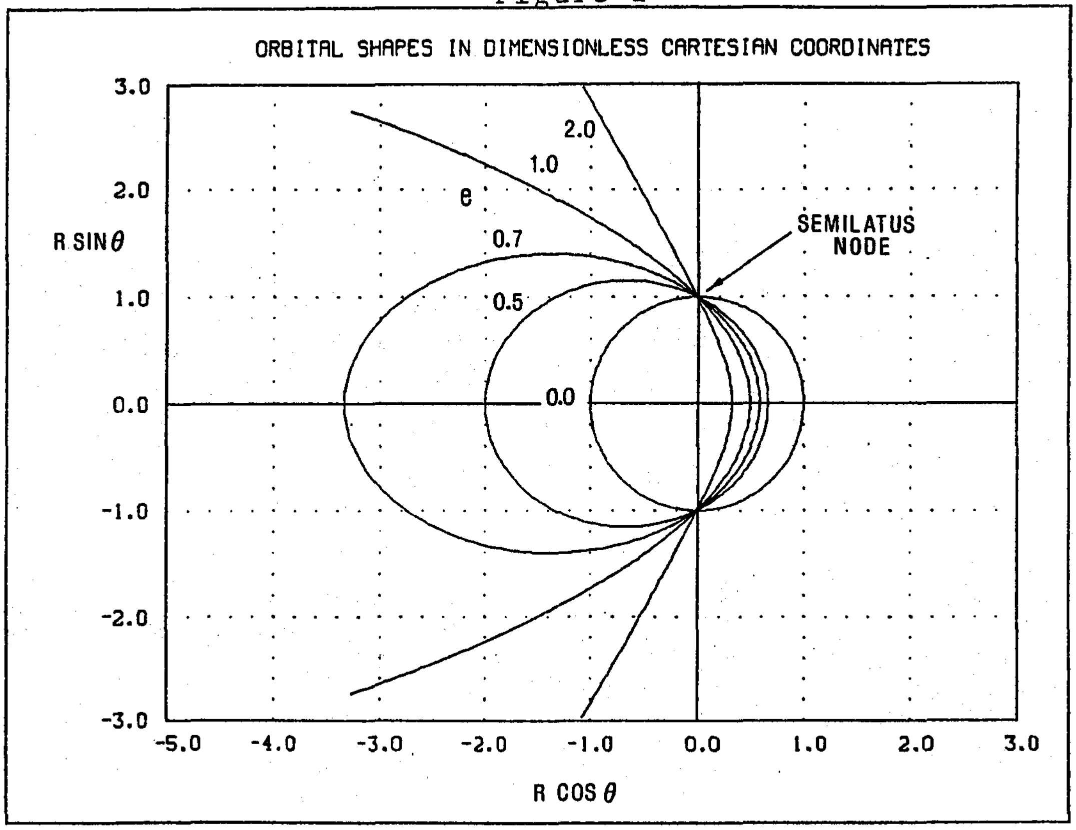

Figure 3

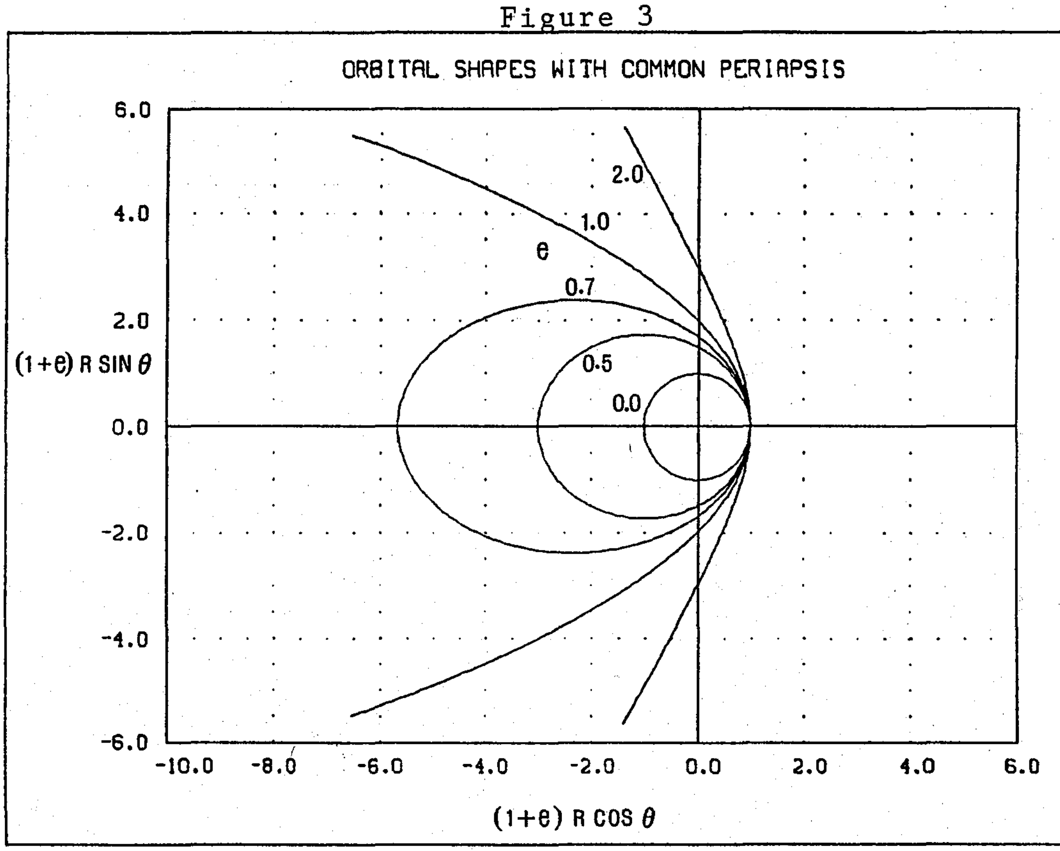

Figure 4

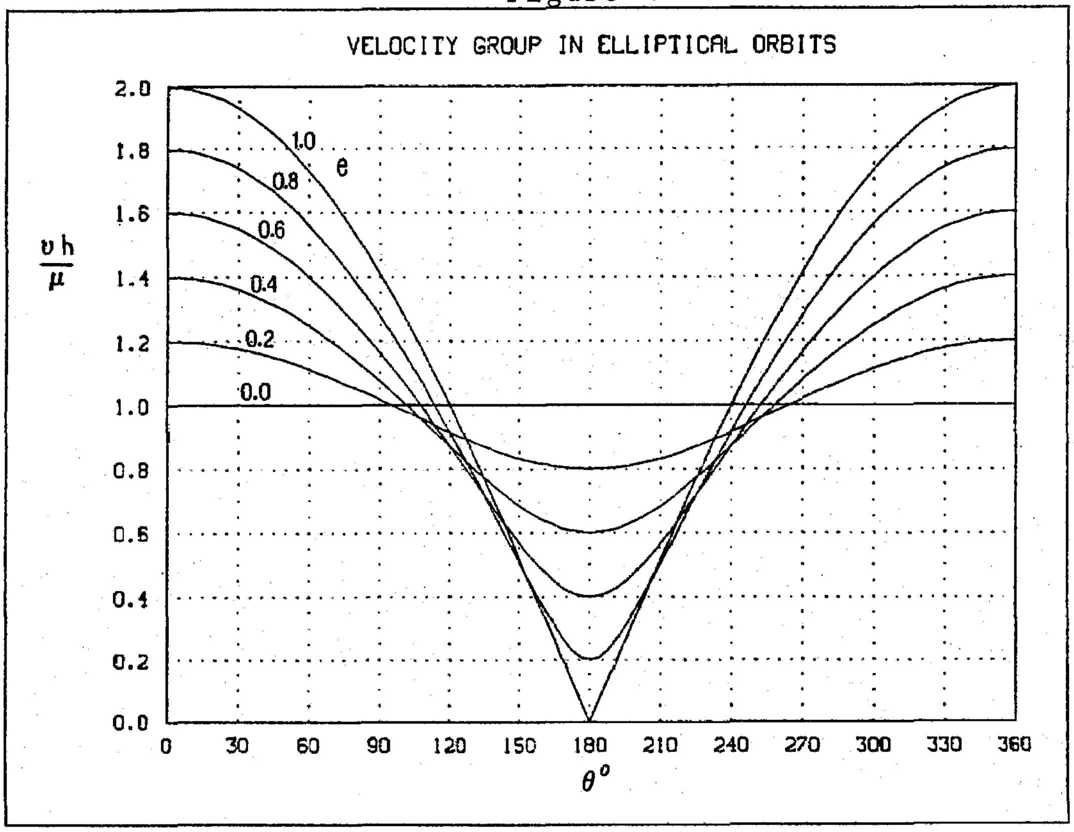

Figure 5

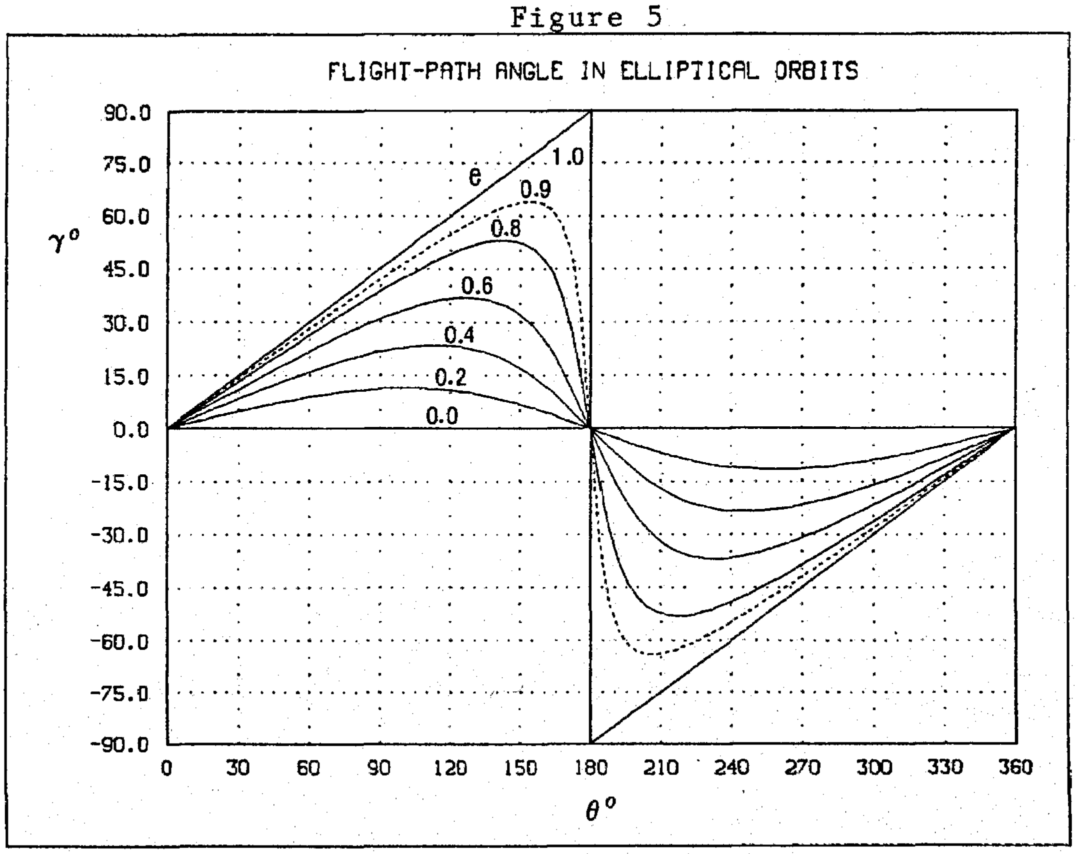

Figure 6

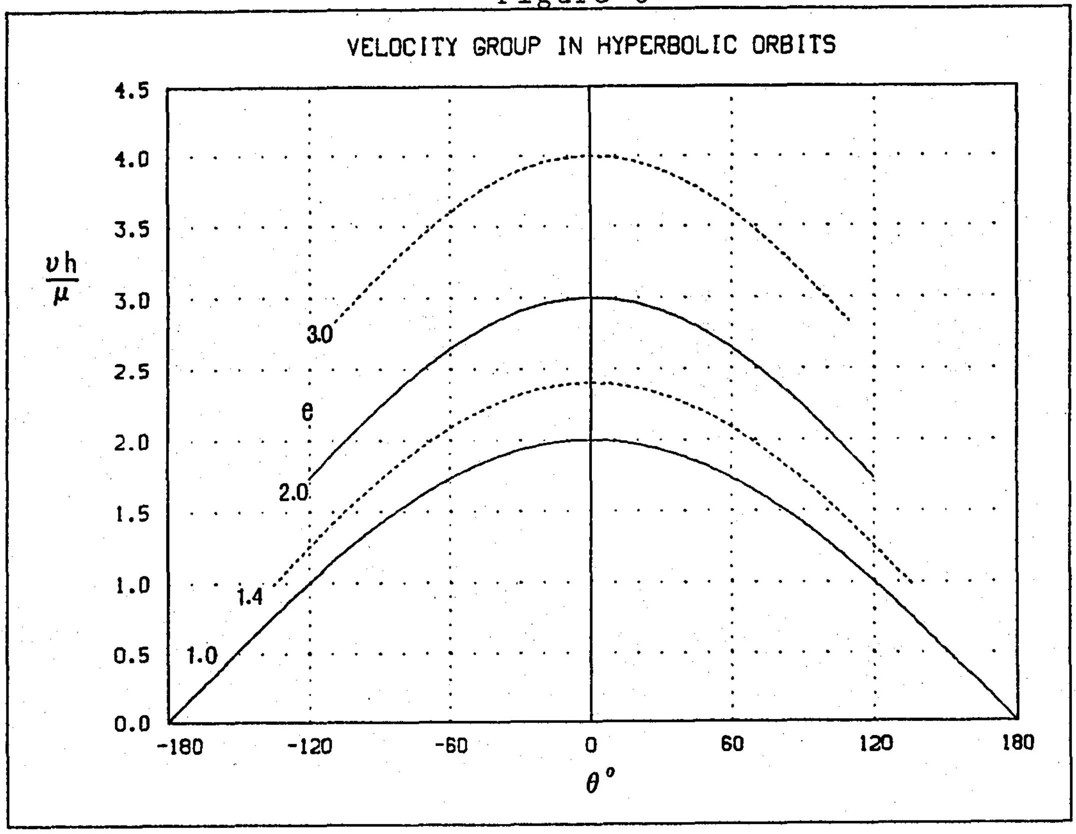

Figure 7

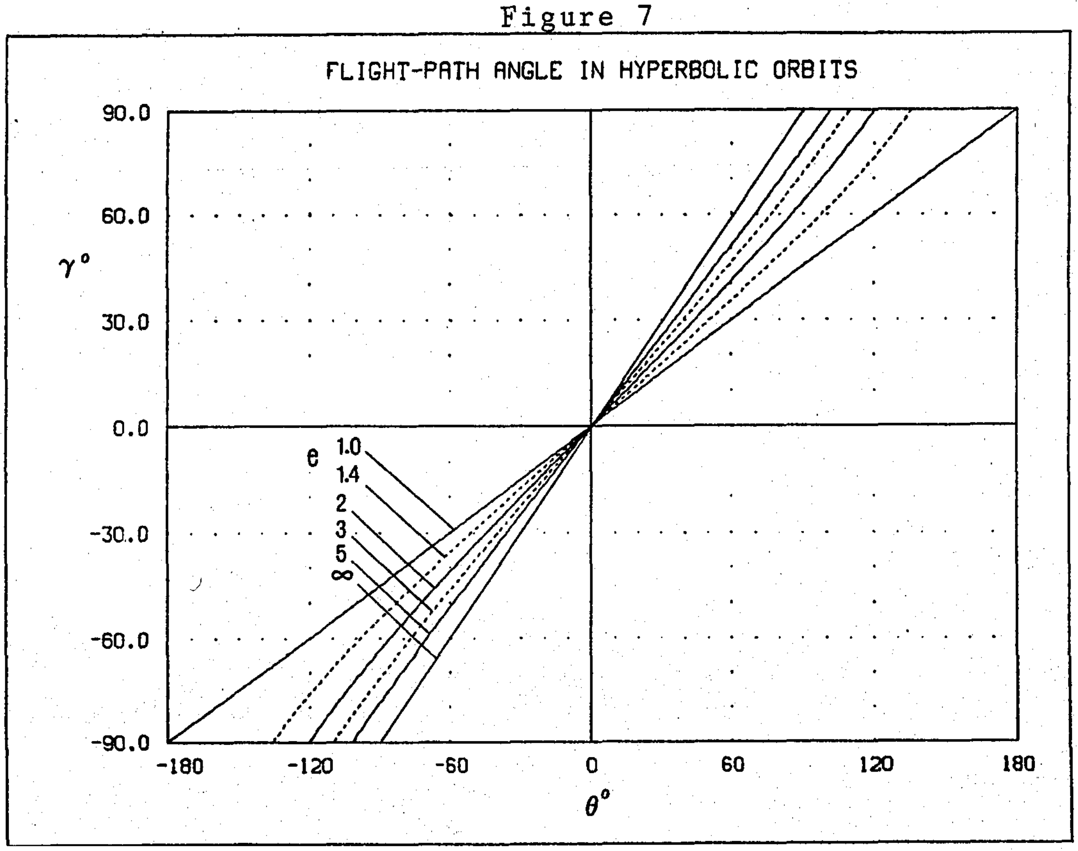

Figure 8

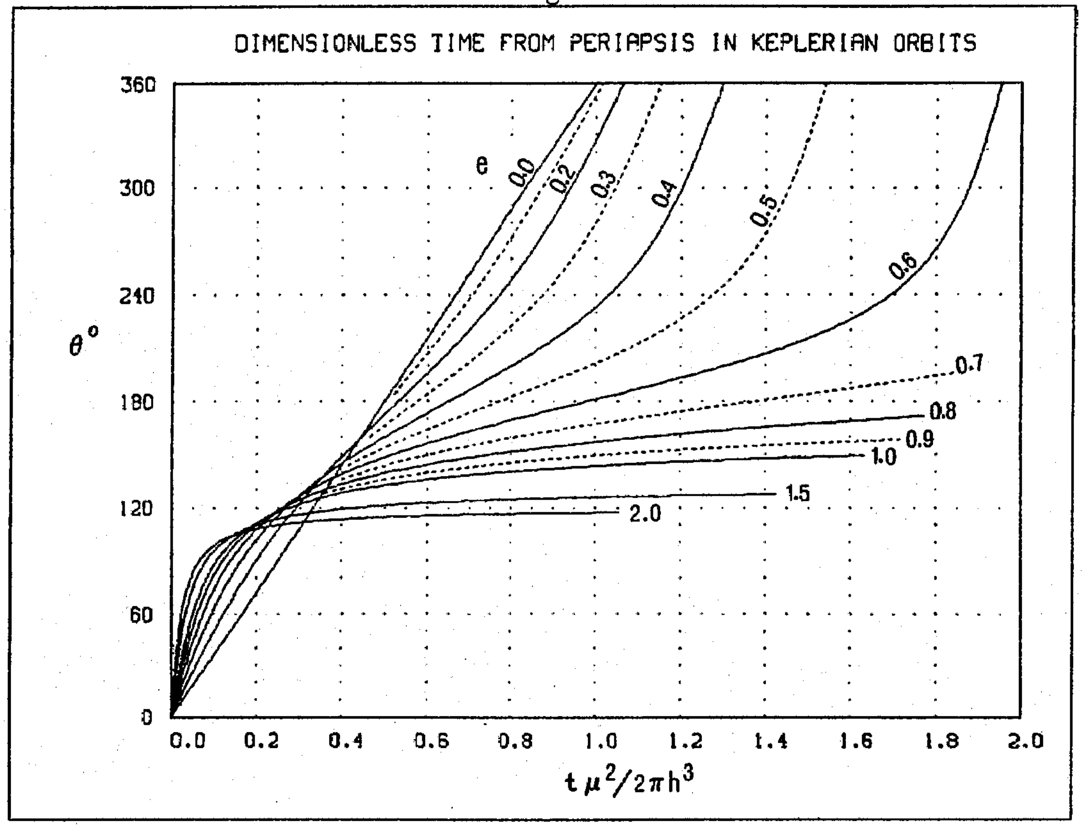

Figure 9

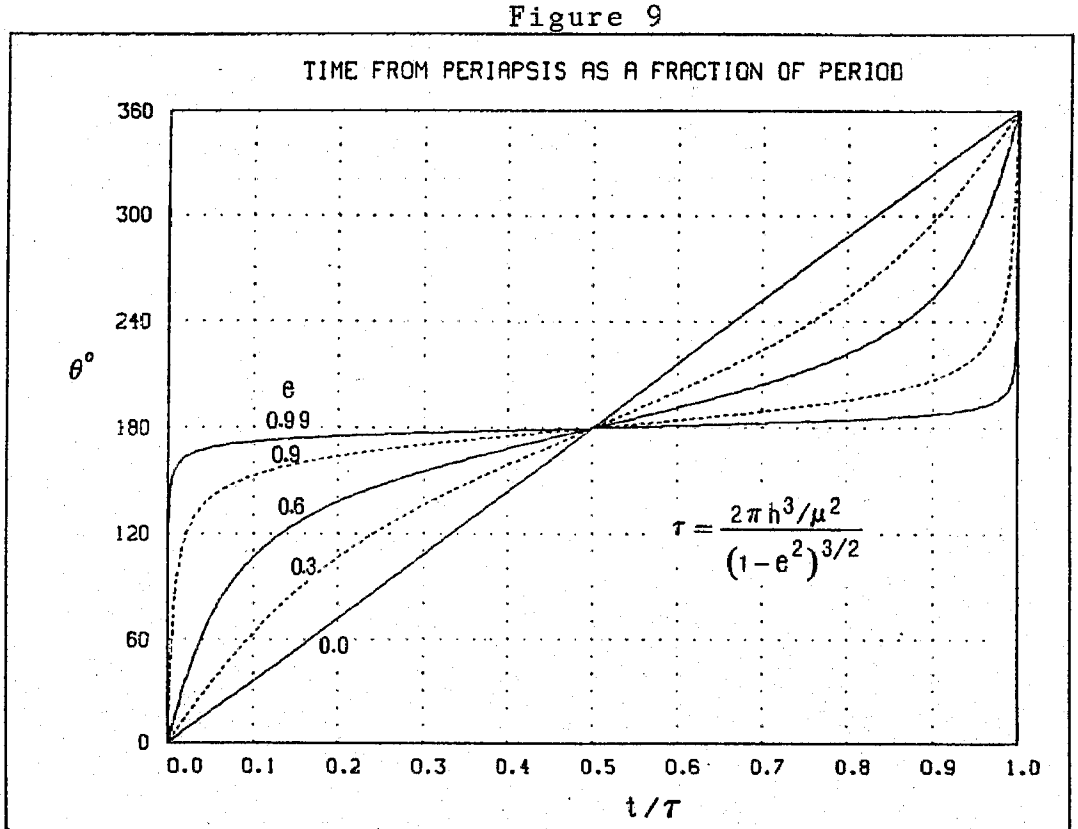

Figure 10

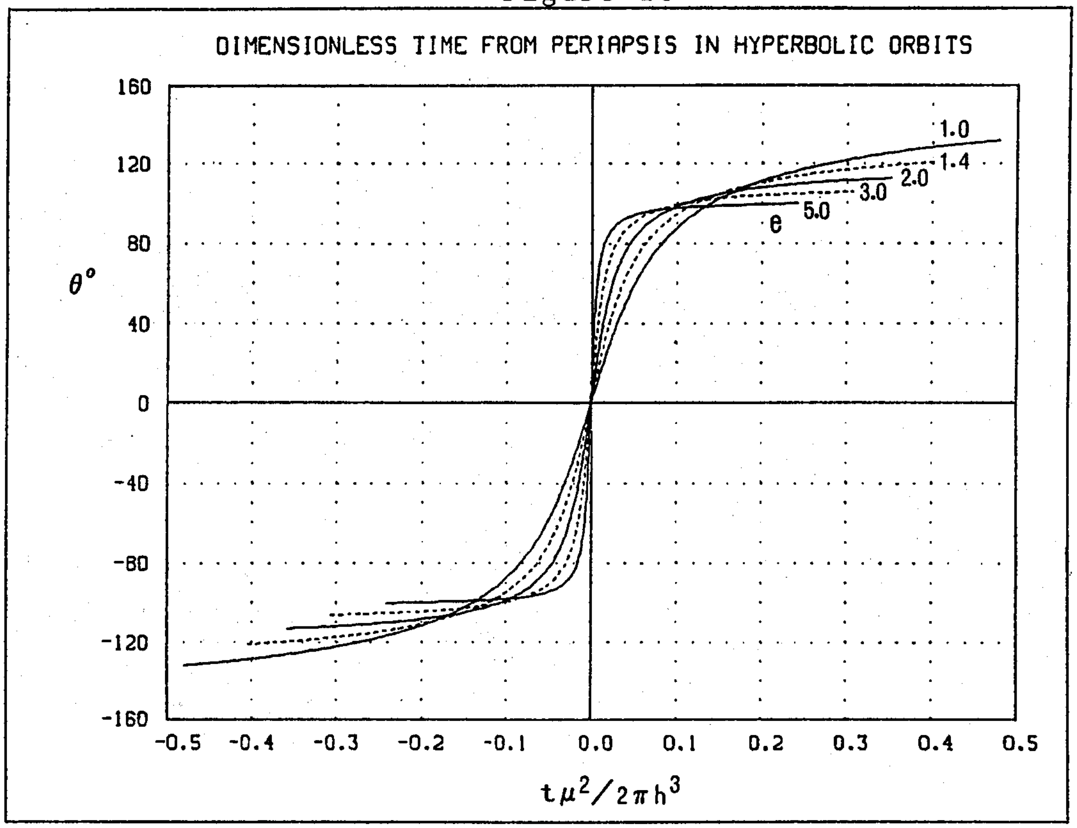

NUMERICAL SOLUTION OF KEPLER'S PROBLEM

The dimensionless time (T) from periapsis to any true anomaly (θ) is given by:

$$T = t\mu^2/2\pi h^3 = (1/2\pi)\int_0^{\theta} \frac{d\theta}{(1+e\cos\theta)^2}$$

The integral can be evaluated numerically, with Simpson's Rule for example, to determine (T), given (e) and (θ). The result can be used to check the accuracy of (T) as determined by the auxiliary anomalies. Alternatively, the equation above can be differentiated and rearranged to yield the dimensionless time derivative:

$$d\theta/dT = 2\pi(1+e\cos\theta)^2$$

This derivative can be used to numerically solve Kepler's problem with a constant or variable time group increment (ΔT). In Table 1, the Runge-Kutta method (Appendix 3) was used with variable (ΔT) adjusted to advance roughly $1°\approx(\theta_{i+1}-\theta_i)$ in true anomaly at each step:

$$\Delta T = T_{i+1}-T_i = 1°(2\pi/360°)/[2\pi(1+e\cos\theta_i)^2]$$

The actual advance $(\theta_{i+1}-\theta_i)$ was calculated in double precision with the Runge-Kutta method. Then, given (θ), the auxiliary anomaly was used to calculate (T) in double precision, thereby obtaining a comparison of the methods at each step.

Table 1
Time Group Comparison
Double Precision

e	$\theta°$ TRUE ANOMALY	$T = t\mu^2/2\pi h^3$ NUMERICAL * INTEGRATION	AUXILIARY ANOMALY
0.6	44.8852	.0527286	.0527286
0.6	89.5376	.1377633	.1377632
0.6	178.619	.9525895	.9525893
0.6	181.619	1.004654	1.004654
0.99	44.8450	.0350285	.0350284
0.99	89.3285	.1048998	.1048998
0.99	136.083	.5895153	.5895152
0.99	169.745	21.21108	21.21114
0.99	180.815	200.6112	200.6123
0.999	44.8443	.0347316	.0347316
0.999	137.975	.6735287	.6735285
0.999	170.263	40.55587	40.55624
0.999	176.669	615.5090	615.7290
0.999	178.914	2885.342	2888.557
0.999	180.767	7605.110	7608.113
1.0	59.7174	.0507011	.0507011
1.0	123.518	.3193351	.3193350
1.0	165.897	14.65918	14.65920
1.0	174.244	210.3356	210.3592
1.001	59.7172	.0506562	.0506562
1.001	123.516	.3195205	.3195204
1.001	165.870	15.13996	15.13998
1.001	170.160	46.13354	46.13406
2.0	59.6042	.0244402	.0244402
2.0	93.7751	.0778429	.0778429
2.0	116.732	.8392446	.8392227

* VARIABLE TIME GROUP INCREMENT $\Delta T = 1°/(d\theta/dT)$

The results of the numerical integration are seen to agree with those of the auxiliary anomaly generally to five or more significant digits, except at the far side of a highly-eccentric orbit ($e \approx 0.999$, $\theta \approx 180°$) where the methods differ at the fourth significant digit. All computations in Table 1 are non-iterative. The computations using the auxiliary anomaly were non-iterative because (θ) was specified. If, however, (T) were specified and (θ) were to be iteratively determined, convergence on (θ) may not be reliable when using the auxiliary anomaly at near-parabolic eccentricity. In this case, numerical integration offers a reliable, non-iterative solution for (θ) accurate to a small fraction of 1°.

When computations are limited to single precision, the numerical integration is frequently more accurate than the auxiliary anomaly at near-parabolic eccentricity. Table 2 presents an accuracy comparison, using the auxiliary anomaly in double precision as the standard of accuracy, and dots to indicate the more accurate values of (T).

TABLE 2
TIME GROUP ACCURACY COMPARISON
SINGLE PRECISION

e	$\theta°$ TRUE ANOMALY	$\tau = t\mu^2/2\pi h^3$ NUMERICAL INTEGRATION *	AUXILIARY ANOMALY	EXACT **
0.99	9.9926	0.007044	0.007044	0.007044
0.99	59.718	0.051152 •	0.051148	0.051152
0.99	120.62	0.281475	• 0.281471	0.281469
0.99	175.12	67.19261	• 67.19213	67.19140
0.99	179.80	172.7628	• 172.7603	172.7578
0.999	9.9926	0.006981 •	0.006978	0.006981
0.999	59.717	0.050745 •	0.050749	0.050745
0.999	119.63	0.271576 •	0.271621	0.271571
0.999	170.26	40.52766 •	40.53115	40.52691
0.999	178.15	1678.677	• 1680.191	1680.005
0.999	180.76	7596.878	• 7599.535	7599.068
1.0	29.931	0.021778	0.021778	0.021778
1.0	90.305	0.106958	• 0.106957	0.106957
1.0	150.31	1.725030	• 1.724981	1.724975
1.0	175.71	509.8093	• 509.9658	509.9817
1.01	4.9982	0.003440 •	0.003383	0.003440
1.01	29.931	0.021567 •	0.021575	0.021567
1.01	90.300	0.106311 •	0.106314	0.106310
1.01	150.24	1.840474	• 1.840397	1.840426
1.01	170.84	289.2851	• 289.7937	289.7665
1.001	9.9926	0.006967 •	0.006961	0.006967
1.001	29.931	0.021757 •	0.022442	0.021757
1.001	60.707	0.051882 •	0.052735	0.051882
1.001	90.305	0.106893 •	0.107820	0.106892
1.001	120.60	0.282638 •	0.283232	0.282631
1.001	150.30	1.735943 •	1.736358	1.735899
1.001	170.15	46.09414	• 46.09236	46.09021
1.001	175.49	693.5461	• 694.2402	693.9728

* VARIABLE TIME GROUP INCREMENT

** AUXILIARY ANOMALY IN DOUBLE PRECISION

ORBIT ANALYSIS WITH THE DIMENSIONLESS GROUPS

To illustrate the application of the dimensionless groups, a lunar free-return trajectory (Figure 11) will be analyzed with the patched-conic method (Ref. 2). The free-return trajectory is useful in the event that the decelerating impulse is not available at perilune, because lunar gravity will then swing the spacecraft into a trajectory returning to the same perigee altitude as the outbound trip.

The patched-conic method can be used for approximate analysis of the free-return trajectory. With this method, the trajectory is analyzed by patching together the various 2-body (conic) orbits, neglecting the effects of third bodies. In the lunar free-return trajectory, only the earth's gravity ($\mu_{\oplus}$=398601 km^3/s^2) is considered until the spacecraft enters the lunar sphere of influence at a distance (r_{im}=66300 km) from the moon. Within the lunar influence sphere (μ_m=4903 km^3/s^2), the effects of the earth on the moon-relative trajectory are neglected. Furthermore, the effects of the sun are neglected in both patched orbits.

Figure 11
Lunar Free-Return Trajectory

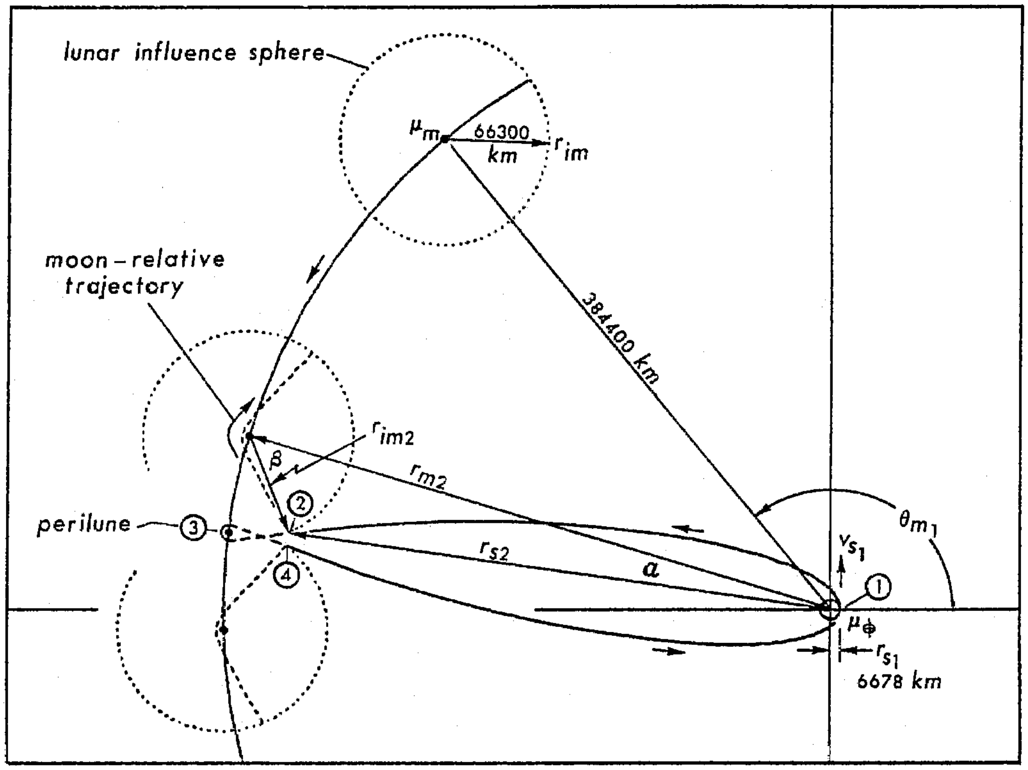

The spacecraft is injected at point (1) from a geocentric parking orbit of 300 km altitude into a highly-eccentric transfer crossing in front of the moon's path. At point (2) the spacecraft enters the lunar influence sphere, beginning its moon-relative hyperbolic encounter. The spacecraft reaches perilune at point (3) and then leaves the lunar influence sphere at point (4). The objectives are to determine the injection speed (v_{s1}), phase angle (θ_{m1}), time (t_{13}) to perilune, and perilune altitude, all such that the earth-relative eccentricity and energy of the return trip match those of the outbound trip.

The analysis begins as recommended in Ref. 1, where both (v_{s1}) and the intercept angle (β) are estimated. These estimates are later revised if the desired trajectory is not observed. From (v_{s1}) and (r_{s1}) the earth-relative angular momentum (h_{12}) is determined. Then the velocity group (V_{s1}) and eccentricity (e_{12}) are determined. From (β, r_{m2}, and r_{im2}) the law of cosines is applied to determine the radius (r_{s2}). Then the radius group (R_{s2}) and true anomaly (θ_{s2}) are calculated:

$$h_{12} = r_{s1}\, v_{s1} \quad \text{(at periapsis)}$$

$$V_{s1} = v_{s1}\, h_{12} / \mu_\oplus$$

$$e_{12} = V_{s1} - 1 \quad \text{(at periapsis)}$$

$$R_{s2} = r_{s2}\, \mu_\oplus / h_{12}^2$$

(11)

$$\theta_{s2} = \cos^{-1}[(1/e_{12})(1/R_{s2}-1)]$$

Next, the velocity group (V_{s2}), velocity (v_{s2}), flight-path angle (γ_{s2}), and velocity vector components are calculated (Refer to Figure 11a):

$$V_{s2} = \sqrt{1+e_{12}^2+2\ e_{12}\cos\theta_{s2}}$$

$$v_{s2} = V_{s2}\mu_\oplus/h_{12}$$

$$\gamma_{s2} = \cos^{-1}(1/R_{s2}V_{s2})$$

$$v_{s2\theta} = v_{s2}\cos\gamma_{s2}; \quad v_{s2r} = v_{s2}\sin\gamma_{s2}$$

$$v_{s2x} = v_{s2r}\cos\theta_{s2} - v_{s2\theta}\sin\theta_{s2}$$

$$v_{s2y} = v_{s2r}\sin\theta_{s2} + v_{s2\theta}\cos\theta_{s2}$$

Figure 11a Velocity Components

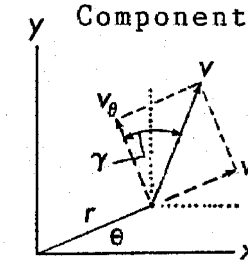

To determine the lunar velocity vector ($\bar{v}_{m2}$) the law of sines is used to determine the angle (α), which is then subtracted from (θ_{s2}) to obtain (θ_{m2}). Then the x-y components of ($\bar{v}_{m2}$) can be determined. The lunar velocity vector is subtracted from the spacecraft velocity vector to obtain the relative velocity vector ($\bar{v}_{s2m}$) with which the spacecraft begins its hyperbolic passage. The lunar influence radius, as a vector ($\bar{r}_{im2}$), is calculated by subtracting the vector ($\bar{r}_{s2}$) from ($\bar{r}_{m2}$) using x-y components ($r\cos\theta$) and ($r\sin\theta$). Finally, the moon-relative angular momentum is found by the vector cross product:

$$\text{vector:}\quad \bar{h}_{24} = \bar{r}_{im2} \times \bar{v}_{s2m}$$

$$\text{scalar:}\quad h_{24} = r_{im2x}\, v_{s2my} - r_{im2y}\, v_{s2mx}$$

The scalar angular momentum (h_{24}) will be negative, provided the spacecraft passes in front of the moon. Taking note of the sign of (h_{24}) for use in subsequent vector rotation operations, its absolute value is used for all remaining calculations. The moon-relative radius group, velocity group, energy group, and eccentricity are as follows:

$$R_{s2m} = r_{im}\mu_m/h_{24}^2$$

$$V_{s2m} = v_{s2m}\, h_{24}/\mu_m$$

$$E_{24} = \tfrac{1}{2}(V_{s2m})^2 - (1/R_{s2m})$$

$$e_{24} = \sqrt{2E_{24}+1}$$

The spacecraft enters the lunar influence sphere with an initial true anomaly:

$$\theta_{s2m} = -\cos^{-1}[(1/e_{24})(1/R_{s2m}-1)]$$

The moon-relative true anomaly (θ_{s4m}) at exit from the lunar influence sphere is positive, with magnitude (θ_{s2m}). Thus, the moon-to-spacecraft radius vector sweeps out an angle ($2\theta_{s4m}$) during hyperbolic passage. This rotation is clockwise, provided the scalar angular momentum (h_{24}) was originally of negative sign. The moon-spacecraft radius vector ($\bar{r}_{im4}$) can thus be determined by rotating the vector ($\bar{r}_{im2}$) clockwise by the angle ($2\theta_{s4m}$).

Figure 12 shows how the new x-y components are determined for a vector which is originally oriented at an angle (ψ) and then rotated clockwise through an angle (δ). When computing (ψ), its quadrant must be taken into account.

Figure 12
VECTOR ROTATION

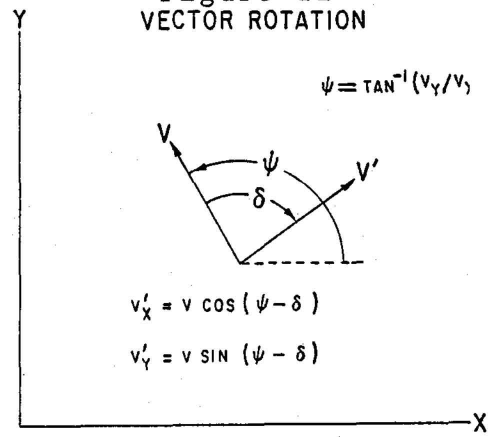

Also during hyperbolic passage, the relative velocity vector is rotated. Again provided the scalar angular momentum (h_{24}) was originally of negative sign, the rotation is clockwise. The relative velocity vector at approach ($\bar{v}_{s2m}$) is thus rotated clockwise to form the relative velocity vector at departure ($\bar{v}_{s4m}$) from the lunar influence sphere. If a spacecraft approaches a central body from a distance of infinity, its relative velocity vector is deflected by an angle

$$\delta_\infty = 2\sin^{-1}(1/e)$$

In a patched-conic condition, however, the radius at approach is finite. Since the central body is "turned off" whenever the spacecraft is outside the influence sphere, the velocity turning angle will be somewhat smaller than (δ_∞). Figure 13 relates the turning angle (δ) to the eccentricity and initial true anomaly, where the turning is limited to that which occurs within the sphere of influence. In the case of the lunar free-return trajectory, the spacecraft enters the lunar influence sphere with (θ=-119.8°) and (e=1.687) as indicated by the dot on the figure. The corresponding turning angle is 72.18°, counter-clockwise in Figure 13, but clockwise in Figure 11 due to the orientation of the hyperbola.

The moon translates during hyperbolic passage. However, the axis of the hyperbola remains fixed in orientation. The time

Figure 13

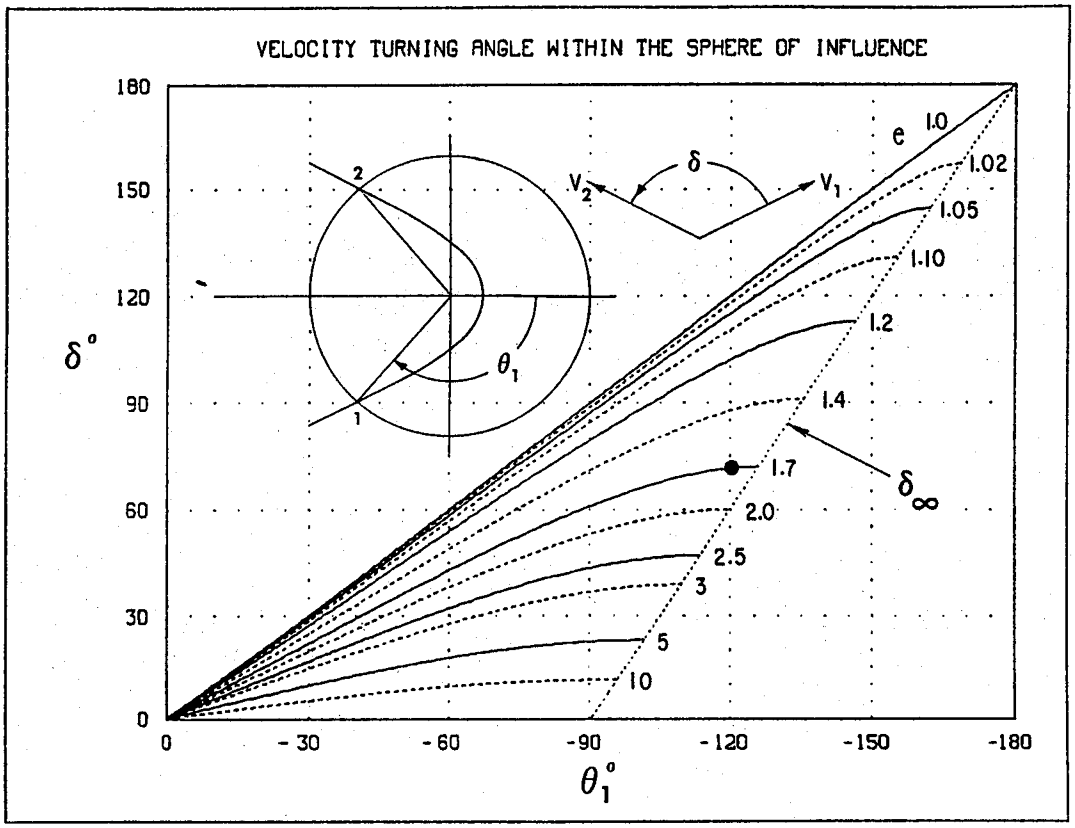

group from perilune at point (3) to point (4) can be doubled to obtain the total dimensionless time in the lunar influence sphere. Then the time is dimensionalized, allowing calculation of the change in the moon's position during hyperbolic passage. The hyperbolic anomaly (F_4) corresponds to the moon-relative true anomaly (θ_{s4m}) and eccentricity (e_{24}).

$$\cosh F_4 = (e_{24} + \cos\theta_{s4m})/(1+e\cos\theta_{s4m})$$

$$\sinh F_4 = \sqrt{\cosh^2 F_4 - 1}$$

$$F_4 = \ln(\cosh F_4 + \sinh F_4)$$

$$T_4 = (e_{24} \sinh F_4 - F_4) \;/\; [2\pi(e_{24}{}^2 - 1)^{3/2}]$$

$$t_{24} = (2T_4)2\pi h_{24}{}^3/\mu_m{}^2$$

$$\theta_{m4} = \theta_{m2} + t_{24}(d\theta/dt)_m$$

Given the moon's true anomaly (θ_{m4}) at the point where the spacecraft leaves the lunar influence sphere, the lunar velocity vector in x-y components can be determined and added to the spacecraft relative velocity vector ($\bar{v}_{s4m}$) to obtain the earth-relative spacecraft velocity vector:

$$\bar{v}_{s4} = \bar{v}_{s4m} + \bar{v}_{m4} \qquad (14)$$

Then the earth-relative spacecraft radius ($\bar{r}_{s4}$) is obtained by adding the earth-moon radius vector ($\bar{r}_{m4}$) to the moon-spacecraft vector ($\bar{r}_{im4}$). Thus the earth-relative angular momentum for the return trajectory is determined by the vector cross product:

$$\bar{h}_4 = \bar{r}_{s4} \times \bar{v}_{s4}$$

The angular momentum is converted to scalar form (h_4) and the earth-relative velocity group, radius group, energy group, and eccentricity for the return trip are calculated:

$$V_{s4} = v_{s4}\, h_4 / \mu_{\oplus}$$

$$R_{s4} = r_{s4}\, \mu_{\oplus} / h_4^{\,2}$$

$$E_4 = \tfrac{1}{2}(V_{s4}^{\,2}) - (1/R_{s4})$$

$$e_4 = \sqrt{2E_4 + 1}$$

Finally, the moon's true anomaly at injection (θ_{m1}) is determined by calculating, and then dimensionalizing, the time group from point (1) to point (2). The resulting time (t_{12}) is added to the time (t_{23}) to determine the outbound time to perilune. At perilune, the altitude is obtained by dimensionalizing the moon-relative radius group:

$$R_{s3m} = 1/(1+e_{24}) \quad \text{at perilune}$$

$$r_{s3m} = R_{s3m}\, h_{24}^{\,2} / \mu_m$$

$$\text{Perilune altitude} = r_{s3m} - 1738 \text{ km}$$

Figure 14 presents the results of the analysis for the proper injection conditions (v_{s1}=10.848 km/s, θ_{m1}=129.61°). As might have been expected, the return trajectory is a mirror image of the outbound trajectory with respect to a line passing through the earth and the point of perilune. When the spacecraft is inside the lunar influence sphere, its earth-relative trajectory completes one end of a distorted "figure-8" shape. Since the axis (A) of the lunar passage hyperbola remains parallel to the line of symmetry, the axis passes through the earth at the point of perilune. Thus, the hyperbolic encounter with the moon does not change the energy of the spacecraft relative to the earth.

The major axis of the outbound elliptical transfer resides on the x-axis. That of the return ellipse (axis B) is inclined to the x-axis. Since the point of injection resides on the x-axis and that of return perigee resides on axis (B), the round trip falls just short of closing the "figure-8" shape.

Figure 14
Injection Conditions and Symmetry
of Lunar Free-Return Trajectory

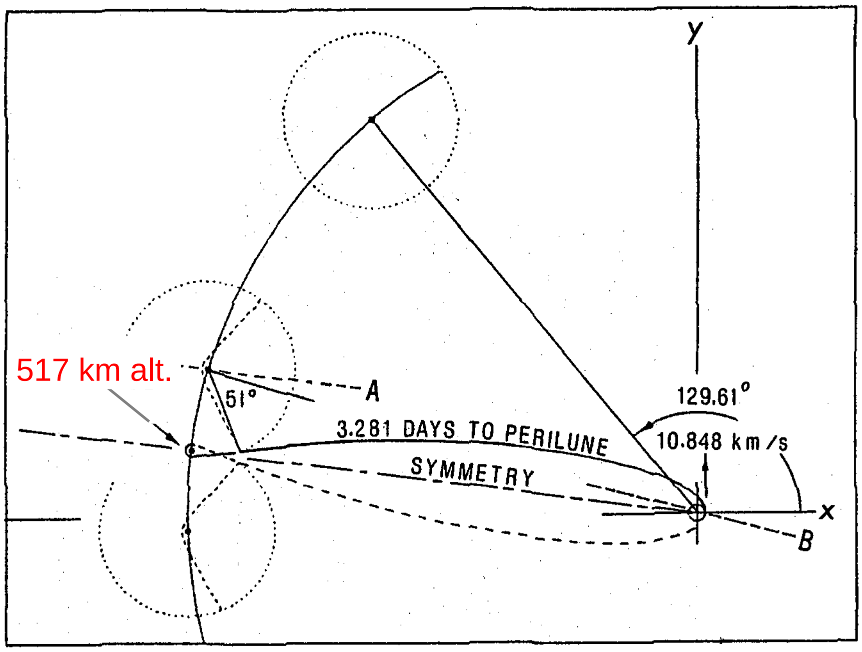

CONCLUSIONS

1. The dimensionless orbital parameters (R,V,E, and T) offer compact mathematical and graphical presentation of Keplerian orbital characteristics, as well as efficient analysis of conic and patched-conic orbits.

2. Numerical solution of Kepler's problem confirms the accuracy of the flight time predicted by the auxiliary anomalies, even at near-parabolic eccentricities.

3. When iterative methods, including those using the auxiliary anomalies, are unable to converge on a solution to Kepler's problem, numerical integration offers a reliable, non-iterative solution.

4. Patched-conic orbits can be conveniently analyzed with the aid of Cartesian vector operations on the dimensional orbital parameters (r) and (v).

REFERENCES

1. Roger Bate, D.Mueller, and J.E.White, Fundamentals of Astrodynamics, Dover Publications, Inc., New York, 1971, pp. 16-29, 187-191.

2. Marshall H. Kaplan, Modern Spacecraft Dynamics and Control, John Wiley & Sons, New York, 1976, pp.91-96.

ACKNOWLEDGEMENT

The following individuals do not necessarily endorse the contents of this paper, but their assistance is greatly appreciated:

Dr. Vladimir Chobotov, of Aerospace Corporation, for a preliminary review and helpful suggestions

David Miller and Wayne Hurwitz, both of Northrop Corp., for development of the computer plotting system used for most of the figures.

APPENDIX 1
DERIVATION OF CONIC-SECTION DIMENSIONLESS PARAMETERS

Conic-Section Orbit Parameters

μ Product of the central-body mass (M) and universal gravitational constant (G)

r Radius from the mass center of the cental body to that of the satellite

θ True anomaly, or angle from closest passage (periapsis)

v Magnitude of the velocity

γ Direction (flight-path angle) of the velocity

h Angular momentum (per unit satellite mass) about the central body

t Time from periapsis to the true anomaly, θ

ε Orbital energy per unit satellite mass

Conic-Section Orbital Equations (Ref. 1, p.16-29, p.187)

1) Radius $r = (h^2/\mu)/(1+e\cos\theta)$

2) Velocity $v = \sqrt{2(\varepsilon + \mu/r)}$

3) Flight-path angle $\gamma = \cos^{-1}(h/rv)$

4) Angular momentum $h = rv \cos \gamma$

5) Energy $\varepsilon = \mu^2(e^2-1)/2h^2 = v^2/2 - \mu/r$

6) Time from periapsis $t = (h^3/\mu^2)\int_0^\theta \frac{d\theta}{(1+e\cos\theta)^2}$

Appendix 1, continued
The Dimensionless Parameters

Equations (1-6) are now manipulated to yield the dimensionless quantities of equations (7-12), using upper-case symbols to designate non-dimensionality:

7) Dimensionless Radius, R $\quad r\mu/h^2 = 1/(1+e\cos\theta)$

8) Dimensionless Velocity, V using (1,2, and 5) $\quad vh/\mu = \sqrt{1+e^2+2e\cos\theta}$

9) Flight-Path Angle, $\quad \cos\gamma = (h/rv) = 1/RV$

10) Dimensionless Angular Momentum, H $\quad RV\cos\gamma = 1$

11) Dimensionless Energy, E using (5) or (7,8) $\quad \varepsilon h^2/\mu^2 = V^2/2 - 1/R = (e^2-1)/2$

12) Dimensionless Time, T from Periapsis $\quad t\mu^2/2\pi h^3 = (1/2\pi)\displaystyle\int_0^\theta \frac{d\theta}{(1+e\cos\theta)^2}$

13) Differentiate (12): $\quad d\theta/dT = 2\pi(1+e\cos\theta)^2$

Relate (T) to the auxiliary anomalies:

14) For $e < 1$,* $\quad T = \dfrac{\epsilon - e\sin\epsilon}{2\pi(1-e^2)^{3/2}} \longrightarrow \left\{ \begin{aligned} \cos\epsilon &= \frac{e+\cos\theta}{1+e\cos\theta} \\ \sin\epsilon &= \frac{\sin\theta\sqrt{1-e^2}}{1+e\cos\theta} \end{aligned} \right.$

15) For $e = 1$,** $\quad T = \dfrac{\tan(\theta/2)}{4\pi} + \dfrac{\tan^3(\theta/2)}{12\pi}$

16) For $e > 1$,** $\quad T = \dfrac{e\sinh F - F}{2\pi(e^2-1)^{3/2}} \longrightarrow \left\{ \begin{aligned} \cosh F &= \cos\epsilon \\ \sinh F &= \sqrt{\cosh^2 F - 1} \\ F &= \ln\left(\cosh F + \sinh F\right) \end{aligned} \right.$

* For $\theta > \pi$, add to T the dimensionless period, $1/(1-e^2)^{3/2}$

** For e=1 or e>1, and θ negative, use positive θ and take the time as negative

APPENDIX 2
Application of the Dimensionless Groups Toward The Iterative Solution of Kepler's Problem

Consider a satellite with velocity (v_o)=4 km/s at a flight-path angle (γ_o)=-60° and radius (r_o)=50,000 km from a central body with gravitational parameter (μ)=400,000 km^3/s^2. Determine the position and velocity one hour later (subscript$_1$).

1) $h = r_o v_o \cos\gamma_o = 100{,}000\ \text{km}^2/\text{s}^2$

2) $V_o = v_o h/\mu = 1$

3) $R_o = r_o\mu/h^2 = 2$

4) $E = \frac{1}{2}(V_o^{\,2})-(1/R_o) = 0$

5) $e = \sqrt{2E+1} = 1$

6) $\theta_o = \cos^{-1}[(1/e)(1/R_o - 1)] = -120°$ (approaching periapsis)

7) $T_o = -0.275665$ from Appendix 1, Eq.(15)

8) $T_1 - T_o = (t_1 - t_o)\mu^2/2\pi h^3 = 0.091674$

9) To solve for the final true anomaly (θ_1) a first guess may be taken from Figure 10. The guess is designated θ_1'

   $\theta_1' = -110°$ based on $T_1 = -0.275665 + 0.091674 = -0.183991$

10) The corresponding time group, $T_1' = -0.190914$ from Eq.(15)

11) The desired value of T_1' is $T_1 = -0.183991$
    Thus, the estimate θ_1' must be revised. The new guess is calculated from the local derivative $(d\theta/dT)$ at θ_1':

$$\theta_1' = \theta_1' + (d\theta/dT)(T_1 - T_1')$$

where $\quad d\theta/dT = 2\pi(1+e\cos\theta_1')^2(360°/2\pi) = 155.857°$

$$\theta_1' = -110° + 155.857°[-.183991-(-.190914)]$$
$$= -108.921°$$

12) Repeat steps (10) and (11) for the following:

   $T_1' = -0.184173 \quad d\theta/dT = 164.383° \quad \theta_1' = -108.891°$

   $T_1' = -0.183991$ ✓ Thus, $\theta_1 = -108.891°$

13) Finally, $V_1 = \sqrt{1+e^2+2e\cos\theta_1} = 1.16295 \quad v_1 = V_1\mu/h = 4.6518$ km/s

   $R_1 = 1/(1+e\cos\theta_1) = 1.47879 \quad r_1 = R_1 h^2/\mu = 36970$ km

   $\gamma_1 = \cos^{-1}(1/R_1V_1) = -54.445°$

APPENDIX 3
Application of Runge-Kutta Numerical Integration to the Solution of Kepler's Problem

Given the eccentricity (e), angular momentum (h), and initial true anomaly (θ_o) in a conic orbit, the change in orbital position during a time interval (t_1-t_o) can be determined by numerical integration of the dimensionless derivative:

$$d\theta/dT = 2\pi(1+e\cos\theta)^2$$

Working with degrees, rather than radians, this becomes:

$$d\theta/dT = 2\pi(1+e\cos\theta)^2(360°/2\pi) = 360°(1+e\cos\theta)^2$$

The time interval is non-dimensionalized as follows:

$$T_1-T_o = (t_1-t_o)\,\mu^2/2\pi h^3$$

Ordinarily, the time datum is zero at periapsis. However, the datum may arbitrarily be set to zero at the initial true anomaly. Then the numerical integration over (T) is terminated when (T) reaches (T_1-T_o). The time group interval (T_1-T_o) may be broken into constant or variable increments of (ΔT). For a given integration step, the gain ($\Delta\theta$) in true anomaly is calculated with the Runge-Kutta method as follows:

$$\Delta\theta_a^\circ = (d\theta/dT)_a^\circ\,\Delta T = 360°(1+e\cos\theta_a)^2\,\Delta T\ ^*$$

$$\theta_b = \theta_a + \tfrac{1}{2}\Delta\theta_a$$

$$\Delta\theta_b = (d\theta/dT)_b\,\Delta T = 360°(1+e\cos\theta_b)^2\,\Delta T$$

$$\theta_c = \theta_a + \tfrac{1}{2}\Delta\theta_b$$

$$\Delta\theta_c = (d\theta/dT)_c\,\Delta T = 360°(1+e\cos\theta_c)^2\,\Delta T$$

$$\theta_d = \theta_a + \Delta\theta_c$$

$$\Delta\theta_d = (d\theta/dT)_d\,\Delta T = 360°(1+e\cos\theta_d)^2\,\Delta T$$

Finally, $\Delta\theta = (1/6)(\Delta\theta_a + 2\Delta\theta_b + 2\Delta\theta_c + \Delta\theta_d)$

At the very first step, $\theta_a = \theta_o$ and on the next step, $\theta_a = \theta_o + \Delta\theta$. At the end of the very last step, $\theta_a + \Delta\theta = \theta_1$

*Computer evaluation of the cosine requires that (θ) be in radians.